Distal and Proximal Ligand Interactions in Heme Proteins: Correlations between C–O and Fe–C Vibrational Frequencies, Oxygen-17 and Carbon-13 Nuclear Magnetic Resonance Chemical Shifts, and Oxygen-17 Nuclear Quadrupole Coupling Constants in $C^{17}O$- and ^{13}CO-Labeled Species†

Ki Deok Park, Kermin Guo, Foluso Adebodun, Mark L. Chiu, Stephen G. Sligar, and Eric Oldfield*
School of Chemical Sciences, University of Illinois at Urbana—Champaign, 505 South Mathews Avenue, Urbana, Illinois 61801
Received June 11, 1990; Revised Manuscript Received November 9, 1990

ABSTRACT: We have obtained the oxygen-17 nuclear magnetic resonance (NMR) spectra of a variety of $C^{17}O$-labeled heme proteins, including sperm whale (*Physeter catodon*) myoglobin, two synthetic sperm whale myoglobin mutants (His E7 → Val E7; His E7 → Phe E7), adult human hemoglobin, rabbit (*Oryctolagus cuniculus*) hemoglobin, horseradish (*Cochlearia armoracia*) peroxidase (E.C. 1.11.1.7) isoenzymes A and C, and *Caldariomyces fumago* chloroperoxidase (E.C. 1.11.1.10), in some cases as a function of pH, and have determined their isotropic ^{17}O NMR chemical shifts, δ_i, and spin–lattice relaxation times, T_1. We have also obtained similar results on a picket fence prophyrin, [5,10,15,20-tetrakis($\alpha,\alpha,\alpha,\alpha$-pivalamidophenyl)porphyrinato]iron(II) (1-MeIm)CO, both in solution and in the solid state. Our results show an excellent correlation between the infrared C–O vibrational frequencies, ν(C–O), and δ_i, between ν(C–O) and the ^{17}O nuclear quadrupole coupling constant (e^2qQ/h, derived from T_1), and as expected between e^2qQ/h and δ_i. Taken together with the work of others on the ^{13}C NMR of ^{13}CO-labeled proteins, where we find an excellent correlation between $\delta_i(^{13}C)$ and ν(Fe–C), our results suggest that IR and NMR measurements reflect the same interaction, which is thought to be primarily the degree of π-back-bonding from Fe d to CO π^* orbitals, as outlined previously [Li, X.-Y., & Spiro, T. G. (1988) *J. Am. Chem. Soc. 110*, 6024]. The modulation of this interaction by the local charge field of the distal heme residue (histidine, glutamine, arginine, and possibly lysine) in a variety of species and mutants, as reflected in the NMR and IR measurements, is discussed, as is the effect of cysteine as the proximal heme ligand.

The nature of Fe–CO (and, in general, Fe–ligand) bonding in heme proteins has been the subject of interest for a number of years (Pauling & Coryell, 1936). There has been considerable interest in investigating these interactions by using vibrational spectroscopy, where C–O stretching frequencies, ν(C–O), Fe–C vibrational frequencies, ν(Fe–C), and Fe–C–O deformations, δ(Fe–C–O), have all been determined in systems such as various myoglobins, hemoglobins, and peroxidases (Ormos et al., 1988; Alben et al., 1982; Yu et al., 1983; Morikis et al., 1988; Choc & Caughey, 1981; Uno et al., 1985, 1987; Anzenbacher et al., 1989; Tucker et al., 1978; Barlow et al., 1976; Evangelista-Kirkup et al., 1986; O'Keefe et al., 1978; Ramsden & Spiro, 1989; Morikis et al., 1989). More recently, the results of nuclear magnetic resonance (NMR) spectroscopic techniques on ^{13}C (Moon & Richards, 1972a,b; Matwiyoff & Needham, 1972; Matwiyoff et al., 1973; Moon et al., 1977; Maciel et al., 1980; Caughey et al., 1981; Behere et al., 1985), ^{17}O (Lee et al., 1988; Lee & Oldfield, 1989), and ^{57}Fe NMR (Lee et al., 1985; Baltzer et al., 1985; La Mar et al., 1985; Baltzer, 1987; Morishima et al., 1989) have been applied to these systems, and we believe that considerable new data on Fe–ligand bonding is likely to be obtained from additional NMR investigations. For example, as shown in Figure 1A, there are in principle at least 14 independent NMR parameters required to fully describe the NMR behavior of an Fe–CO fragment [the principal elements of the ^{57}Fe chemical shift tensor $\delta_{11}(^{57}Fe)$, $\delta_{22}(^{57}Fe)$, and $\delta_{33}(^{57}Fe)$; the principal elements of the ^{13}C chemical shift tensor, $\delta_{11}(^{13}C)$, $\delta_{22}(^{13}C)$, and $\delta_{33}(^{13}C)$; the principal elements of the ^{17}O chemical shift tensor, $\delta_{11}(^{17}O)$, $\delta_{22}(^{17}O)$, and $\delta_{33}(^{17}O)$; the principal elements of the ^{17}O electric field gradient tensor, $V_{xx}(^{17}O)$, $V_{yy}(^{17}O)$, and $V_{zz}(^{17}O)$] together with three scalar couplings (direct dipolar couplings are not considered since they are expected to be very difficult to determine). For an Fe–O_2 fragment, there are at least 16 independent NMR parameters, Figure 1B. There are thus a total of 30 NMR parameters that might be extracted from NMR measurements on Fe–CO and Fe–O_2 fragments in heme proteins and model systems, versus six that have been determined to date from vibrational spectroscopy. It is our belief that any additional information obtainable from NMR spectroscopy will be a welcome complement to existing vibrational spectroscopic data, since [together with theoretical developments; see, e.g., Augspurger et al. (1990)] it should help provide a more complete analysis of the nature of Fe–ligand bonding. We should say at once that considerable further advances in both theory *and* experiment will be required in order to carry out such detailed analyses, but the point remains that NMR studies of ^{13}C, ^{17}O, and ^{57}Fe appear, at the very least, to be promising developing techniques with which to probe structure and bonding in metalloproteins. We try to build on this assertion in this paper.

At present, it is not possible to determine all chemical shift and field gradient tensor elements in proteins. Rather, we believe that the results published to date, together with unpublished results (on ^{57}Fe; J. C. Chung, H. C. Lee, and E. Oldfield, unpublished results) and those presented herein, indicate that ~12 independent values may be obtained in heme proteins or their model systems. These are the isotropic chemical shift (δ_i) and shift tensor anisotropy ($\Delta\delta$) for ^{13}C; δ_i and $\Delta\delta$ for ^{57}Fe; δ_i and the nuclear quadrupole coupling constant (e^2qQ/h) for $C^{17}O$; δ_{11}, δ_{22}, and δ_{33} for Fe–$^{17}O_2$ (both oxygens, in a model "picket fence" porphyrin; H. C. Lee, C. Coretsopoulos, K. P. Park, F. Adebodun, and E. Oldfield,

† This work was supported by the U.S. Public Health Service (Grant NIH HL-19481).

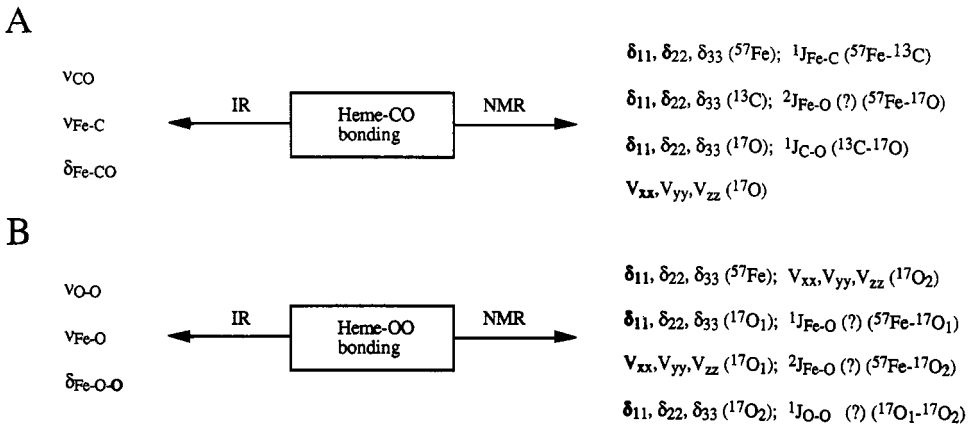

FIGURE 1: NMR and vibrational spectroscopic parameters that might be used to investigate ligand binding in heme proteins.

unpublished results); and δ_{11}, δ_{22}, and δ_{33} for Fe–C^{17}O (again, in a picket fence porphyrin), together with upper limits for e^2qQ/h for both oxygens in a picket fence porphyrin (H. C. Lee, C. Coretsopoulos, K. P. Park, F. Adebodun, and E. Oldfield, unpublished results). There are also very good prospects for additional information in the foreseeable future by using, e.g., solid-state NMR of ^{13}C and ^{57}Fe.

In this paper, we report the ^{17}O NMR δ_i values for a range of C^{17}O-labeled heme proteins in solution, as well as T_1 values for the C^{17}O ligand, from which we can estimate e^2qQ/h. We discuss the modulation of these and related (e.g., ^{13}C NMR) parameters by the local environment (or charge field) and comment on the effects seen when modifying this local field (e.g., by protonation, mutation by site-directed mutagenesis, or interspecies variations). We find an interesting correlation between ν(C–O) and $\delta_i(^{17}O)$, between ν(C–O) and the ^{17}O e^2qQ/h, and between δ_i and e^2qQ/h, arguing for a similar "fluctuation" influencing ν(C–O), $\delta_i(^{17}O)$, and $e^2qQ/h(^{17}O)$. The correlations with ν(C–O) are much better than those that can be constructed from ^{13}C NMR measurements, due in part to the much larger chemical shift range for ^{17}O, early problems with ^{13}C referencing standards, and the possibility that ^{17}O is primarily influenced by the local distal charge field interaction. We show, however, that many earlier ^{13}C NMR results on proximal His-containing proteins can be used to predict ν(C–O) values [or in principle $\delta_i(^{17}O)$ or $e^2qQ/h(^{17}O)$]. For example, we predict ν(C–O) for the low-pH form of sperm whale (*Physeter catodon*) MbCO to be $\approx$1969 ± 5 cm^{-1}, close to the observed $\sim$1967 cm^{-1} (Morikis et al., 1989; Ramsden & Spiro, 1989), or predict ν(C–O) for the β chain of hemoglobin Zürich to be at $\simeq$1957 cm^{-1}, again very close to the experimental value of 1958 cm^{-1} (Choc & Caughey, 1981). For the most part, then, ν(C–O), $\delta_i(^{13}C)$, $\delta_i(^{17}O)$, and $e^2qQ/h(^{17}O)$ are all interrelated, and possible reasons for this are discussed. We also note that change in the proximal residue to a mercaptide causes anomalous effects on $\delta_i(^{13}C)$, while $\delta_i(^{17}O)$ is not so affected—and again suggest possible reasons for this. In particular, our observation of a monotonic relation between $\delta_i(^{13}C)$ and ν(Fe–C) in *all* proteins argues strongly for the dominance of metal–carbon π-bonding as the major influence on ^{13}C chemical shifts, while $\delta_i(^{17}O)$ and $e^2qQ/h(^{17}O)$ are affected in a more direct fashion by the nature of the distal charge field. When viewed together, all of the data—$\delta_i(^{17}O)$, $e^2qQ/h(^{17}O)$, $\delta_i(^{13}C)$, ν(C–O), and ν(Fe–C)—can be readily interpreted in terms of a simple model of Fe–C–O π-bonding and back-bonding interactions, as might be anticipated for substituted metal carbonyls (Buchner & Schenk, 1982; Brownlee et al., 1986) and as suggested for many heme proteins by Li and Spiro (1988).

We concentrate in this paper primarily on ^{17}O NMR spectroscopy. There have, to date, been only two ^{17}O NMR studies of heme proteins (Lee et al., 1988; Lee & Oldfield, 1989). This can perhaps be attributed to the expectation that NMR studies of quadrupolar nuclei in proteins would be particularly difficult, due to excessive line broadening due to long rotational correlation times, τ_R. For typical ^{17}O e^2qQ/h values in the range $\approx$5–15 MHz, this would be true, but it is incorrect for C^{17}O-labeled systems, for two reasons. First, C^{17}O e^2qQ/h values in metallocarbonyls are very small—in the range $\sim$0.5–3 MHz, due it is thought to π-back-bonding effects. This can be seen in a semiquantitative fashion by examination of the oxygen 2p orbital occupancies calculated by Case et al. (1979) for HbCO. These workers found the following electronic populations: O_{2p_x} = 1.40, O_{2p_y} = 1.40, and O_{2p_z} = 1.44, leading to a 2p orbital imbalance of $\sim$0.04e. For a single electron imbalance, e^2qQ/h has been determined experimentally to be 20.88 MHz, so a 0.04e unbalance should lead, very crudely, to an $\approx$1 MHz e^2qQ/h—as found experimentally. The second factor leading to narrow-line ^{17}O NMR spectra is that, outside of the "extreme-narrowing" limit, line widths are governed by three exponential terms, with one of these terms yielding a very long T_2. Thus, the combination of a small e^2qQ/h value and slow molecular tumbling permits observation of ^{17}O NMR spectra from C^{17}O ligands in species as large as hemoglobin.

For oxy proteins, the same cannot be said, since e^2qQ/h values, although not in the 10–20-MHz range expected for say O_3, are still sufficiently large to preclude observation of narrow-line ^{17}O spectra. In addition, ligand exchange (in O_2 but not CO proteins) may also play a role in line broadening. These effects may be ameliorated somewhat by observing solid samples, where line broadening is inhomogeneous, rather than homogeneous, as is the case of the liquid-state systems. For inhomogeneous interactions, refocusing (spin–echo) techniques are quite successful in recovering spectral lies up to $\approx$0.1 MHz—much greater than can be observed in solution, by using pulsed NMR techniques.

Thus, ^{17}O NMR appears to be a very useful probe of heme protein structure and bonding, since both chemical shift and quadrupole coupling constant (electric field gradient tensor) information, in suitable cases, may be determined. In the future, the third main gaseous ligand, NO, might also become accessible, as might other important species, such as ferryl (Fe–O) proteins, as well as nonheme proteins (e.g., hemerythrin), and indeed we have already observed ^{17}O resonances from a hemerythrin model compound (K. D. Park, C. Coretsopoulos, H. C. Lee, F. Adebodun, K. Guo, and E. Oldfield, unpublished results).

Experimental Section

Chemical Aspects. The preparation of hemoglobin, myoglobin, chloroperoxidase, and horseradish peroxidase samples for NMR spectroscopy was as described previously (Lee et al., 1988), and most of the experimental results described in this reference are used again in this paper, but with further analysis. Mutant sperm whale myoglobins were prepared by site-directed mutagenesis, by inserting oligonucleotides coding for valine or phenylalanine in place of the distal His E7(64). The synthetic wild-type form has an additional methionine at the amino terminus but shows no difference in optical, Raman, or magnetic spectroscopic behavior (Springer & Sligar, 1987; Braunstein et al., 1988; Morikis et al., 1989).

The carbon monoxide complex of a picket fence porphyrin [[5,10,15,20-tetrakis($\alpha,\alpha,\alpha,\alpha$-*o*-pivalamidophenyl)-porphyrinato]iron(II)] was prepared as described previously (Lee & Oldfield, 1989) from the free prophyrin, purchased from Mid-Century Chemicals (Posen, IL). For the preparation of a powdered sample of Fe($\alpha,\alpha,\alpha,\alpha$-$T_{piv}$pp)(1-MeIm)$C^{17}O$, the $^{16}O_2$ complex of the 1-MeIm picket fence prophyrin was deoxygenated in the solid state by evacuation for several hours at 10^{-4} torr and 25 °C and then carbonylated with $C^{17}O$. $C^{17}O$ was obtained from ICON Services, Inc. (Summit, NJ).

NMR Spectroscopy. ^{17}O NMR spectra were obtained on a "home-built" NMR spectrometer, which consists of an 11.7-T 2.0-in. bore superconducting solenoid magnet (Oxford Instruments, Osney Mead, UK), a Nicolet (Madison, WI) Model 1280 computer system, and an Amplifier Research (Souderton, PA) Model 200L radiofrequency amplifier, together with assorted ancillary digital and radiofrequency electronics. For solution NMR, we used a 10-mm broad-band probe (Cryomagnet Systems, Indianapolis, IN) with a solution volume of ~3 mL. For solid-state NMR, we used a home-built double-bearing probe, having a sample volume of ~100 μL. The 90° pulse widths on the solution probe were ~40 μs. Spin–lattice relaxation times, T_1, were determined by using a 180–τ–90 pulse sequence, exactly on resonance. For solid-state experiments, the 90° pulse width (on H_2O) was ~15 μs. Chemical shifts are reported in parts per million from internal water, except in the case of the picket fence prophyrin, where an external tap-water standard was used. Low-field, high-frequency, paramagnetic or deshielded values are taken to be positive (IUPAC δ-scale). For consistency, we report chemical *shift* tensor elements using the same solution NMR chemical shift convention (as opposed to a shielding convention, in which the signs change).

Results and Discussion

Brief Theoretical Background to NMR Measurements. Before detailing our ^{17}O NMR results, we wish to very briefly comment on the methods used to obtain the ^{13}C, ^{17}O, and ^{57}Fe NMR parameters discussed in the Introduction, since we will be discussing some of them, and their correlations with ν(C–O) and ν(Fe–C), later in this paper and elsewhere.

For carbon-13 NMR, a conventional solution NMR spectrum yields the isotropic chemical shift, δ_i. From T_1, linewidth, or spin–spin (T_2) relaxation measurements, especially as a function of magnetic field strength, H_0, it is possible to determine the anisotropy of the chemical shift tensor, $\Delta\delta$, at least for the case of an axially symmetric chemical shift tensor.

Quite generally (for ^{13}C, ^{17}O, or ^{57}Fe) we can define the isotropic chemical shift, δ_i, the shift anisotropy, $\Delta\delta$, and the asymmetry parameter, η, as

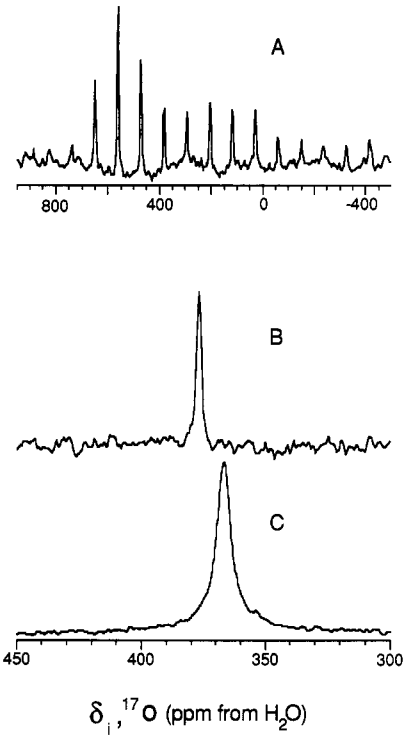

FIGURE 2: Representative ^{17}O NMR spectra of CO–heme systems. (A) $C^{17}O$ picket fence porphyrin in the solid state, magic-angle sample spinning at 4.7 kHz. (B) Same as (A) but sample dissolved in benzene and spectrum recorded by using a conventional high-resolution probe. (C) *P. catodon* carbonmonoxymyoglobin, 13 mM, pH = 7.0, again recorded by using a high-resolution probe.

$$\delta_i = \tfrac{1}{3}(\delta_{11} + \delta_{22} + \delta_{33}) \quad (1)$$

$$\Delta\delta = \delta_{33} - \tfrac{1}{2}(\delta_{11} + \delta_{22}) \quad (2)$$

$$\eta = \frac{\delta_{22} - \delta_{11}}{\delta_{33} - \delta_i} \quad (3)$$

where we have used the convention that $|\delta_{33} - \delta_i| \geq |\delta_{11} - \delta_i| \geq |\delta_{22} - \delta_i|$. For $\delta_{11} = \delta_{22}$, $\eta = 0$ and we define the shift perpendicular to the (CO) symmetry axis as $\delta_\perp = \delta_{11} = \delta_{22}$ and the shift parallel to this axis as $\delta_\parallel = \delta_{33}$. Thus, $\Delta\delta = |\delta_\parallel - \delta_\perp|$. There is in all reported T_1 determinations of $\Delta\delta$ the simplifying assumption, approximately justified, of axial symmetry. Deviation from axial symmetry can, in principle, be assessed via solid-state determinations of the overall shape and breadth of the chemical shift tensor, using "magic-angle" sample spinning methods (Oldfield et al., 1985; Walter et al., 1989).

For ^{57}Fe NMR, we have basically the same situation in that δ_i may be readily determined, while $\Delta\delta$ must be extracted from T_1/T_2/correlation time (τ_R) determinations (Lee et al., 1985; Baltzer et al., 1985; Baltzer, 1987). We believe reasonably accurate $\Delta\delta$ values, and accurate δ_i ones, are currently obtainable for ^{57}Fe. Solid-state measurements (using large samples and cross-polarization) may in the future be possible for solid proteins but are much more likely to be successful for model systems, the largest system studied to date being $[^{57}Fe(bpy)_3]I_2$ (J. C. Chung, H. C. Lee, and E. Oldfield, unpublished results).

For ^{17}O NMR, solution spectra give δ_i, and from T_1 and line width W ($=1/\pi T_2$) or correlation time measurements we can estimate the strength of the major interaction responsible for relaxation, which in this case is *not* the chemical shift anisotropy but, rather, the nuclear quadrupole interaction (Lee & Oldfield, 1989). The derived parameter is the quadrupole

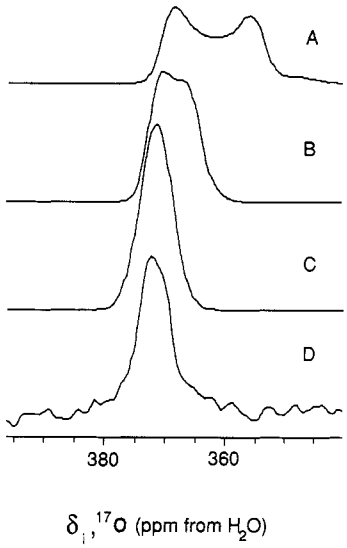

FIGURE 3: e^2qQ/h determination on $C^{17}O$ picket fence porphyrin. (A) Computer simulation of the central ($^1/_2$–$^{-1}/_2$) transition, using e^2qQ/h = 3.0 MHz and a 270 Hz Gaussian line broadening, at 11.7 T. (B) As (A) but e^2qQ/h = 2.0 MHz. (C) As (A) but e^2qQ/h = 1.2 MHz and a 400 Hz line broadening. (D) Experimental spectrum (expansion of center-band peak from Figure 2A).

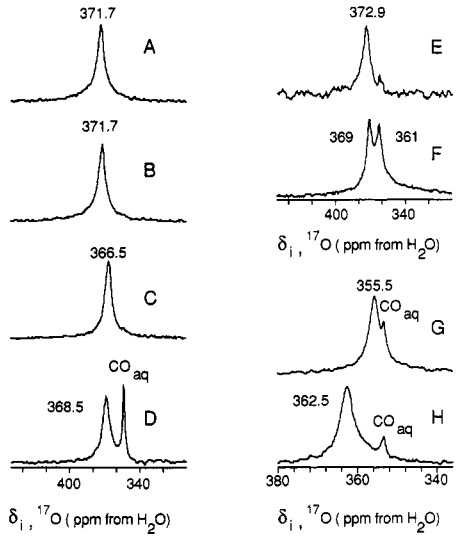

FIGURE 4: Solution-state ^{17}O NMR spectra (11.7 T, 67.8 MHz) of $C^{17}O$–heme proteins. (A) Synthetic *P. catodon* myoglobin His E7 → Val, 5 mM, pH = 7.0, 280 000 accumulations, line broadening = 100 Hz. (B) His E7 → Phe synthetic *P. catodon* myoglobin His E7 → Phe, 5 mM, pH = 7.0, 300 000 accumulations, line broadening = 100 Hz. (C) *P. catodon* myoglobin, 5 mM, pH = 7.0, 300 000 accumulations, line broadening = 100 Hz. (D) *P. catodon* myoglobin, 5 mM, pH = 4.4, 360 000 accumulations, line broadening = 100 Hz. (E) *G. dibranchiata* hemoglobin, 3 mM, pH = 7.2, 150 000 accumulations, line broadening = 100 Hz. (F) Rabbit (*O. cuniculus*) hemoglobin, 2.5 mM in tetramer, pH = 7.0, 280 000 accumulations, line broadening = 100 Hz. (G) Horseradish (*C. armoracia*) peroxidase isoenzyme A (E.C. 1.11.1.7), 1 mM, pH = 9.5, 240 000 accumulations, line broadening = 100 Hz. (H) As (G) but pH = 4.5. The recycle times were typically ~100 ms.

coupling constant, e^2qQ/h. For ^{17}O, we have the following definitions:

$$|V_{zz}| \geq |V_{yy}| \geq |V_{xx}| \quad (4)$$

$$\eta = \frac{V_{xx} - V_{yy}}{V_{zz}} \quad (5)$$

$$e^2qQ/h = eQV_{zz} \quad (6)$$

where V_{ii} are the elements of the electric field gradient tensor, η is the asymmetry parameter, and Q is the nuclear quadrupole moment.

For ^{17}O, we can in some cases also estimate the elements of the chemical shift tensor, δ_{11}, δ_{22}, and δ_{33}, by using magic-angle sample spinning methods, as described herein for a $C^{17}O$ picket fence porphyrin. This is possible because the ^{17}O nuclear quadrupole coupling constant in metal carbonyls is quite small, typically ≈1–3 MHz (Aime et al., 1983, 1984, 1988; Hawkes et al., 1984; Oldfield et al., 1985; Brownlee et al., 1986), due presumably to "back-bonding". In $C^{17}O$ itself, e^2qQ/h is ~+4.4 MHz (Rosenblum & Nethercot, 1957; Richardson, 1960; Lefebvre-Brion et al., 1963; Lovas & Tiemann, 1974; Flygare & Weiss, 1966; Amos, 1979; Cummings et al., 1987), still a very small value compared with most organic carbonyls, in the 10–12 MHz range (Kintzinger, 1981), or the ~16 MHz value found in, e.g., Vaska's compound (Lumpkin et al., 1979). The extremely small e^2qQ/h value makes solution determination of its magnitude feasible and permits solid-state NMR determination of δ_{ii}, the chemical shift tensor, in suitable systems.

Spectroscopic Results

We show in Figure 2A the 11.7-T solid-state magic-angle sample spinning ^{17}O NMR spectrum of $C^{17}O$ picket fence porphyrin, in which we observe only the ($^1/_2$,$^{-1}/_2$) transition, together with an ^{17}O NMR spectrum of the same material in benzene solution (Figure 2B), and for comparison the solution ^{17}O NMR spectrum of sperm whale $MbC^{17}O$ (pH = 7.0, 26 ± 2 °C), Figure 2C.

The solid-state spectrum consists of a center band and a manifold of spinning side bands, from which we can derive the following chemical shift tensor information (Herzfeld & Berger, 1980): $\delta_{11} = \delta_{22}$ = 643 ± 20 ppm, δ_{33} = −171 ± 20 ppm, δ_i = 372 ppm, $\Delta\delta$ = 814 ± 30 ppm. We observe in this case only the central ($^1/_2$,$^{-1}/_2$) transition of the $I = {}^5/_2$ ^{17}O nucleus. The chemical shift anisotropy (CSA) $\Delta\delta$ is larger than that found previously for the group 6 metal carbonyls (619–691 ppm; Oldfield et al., 1985). In solution, rapid molecular tumbling averages the chemical shift (and quadrupolar) interactions, and only a single line representing all spin transitions is observed, at $\delta_i \simeq (\delta_{11} + \delta_{22} + \delta_{33})/3$ or in this case at 376 ppm, in benzene. The line width in solution is quite narrow and is due primarily to relaxation from the quadrupolar interaction. A similar relatively narrow line is found for sperm whale MbCO, Figure 2C. This at first glance could appear surprising, since the correlation time for MbCO is expected to be much longer than that of the model system. However, as we discuss in detail elsewhere (Lee & Oldfield, 1989), the decay of both transverse and longitudinal magnetization in the slow-motion limit (experienced by MbCO) is a weighted sum of three exponentials, and the width at half-height is dominated by a long-T_2 component; i.e., we observe for proteins primarily a "narrow-line" component (Lee & Oldfield, 1989). If this were not the case, ^{17}O NMR studies of heme proteins would be most difficult.

From the spectrum shown in Figure 2A, we can make an estimate of e^2qQ/h for the $C^{17}O$ oxygen, as shown in Figure 3. Here, we have expanded the center-band resonance for the picket fence porphyrin and show in addition computer simulations of the magic-angle sample spinning ^{17}O NMR line shapes expected for e^2qQ/h = 3.2 and 1.2 MHz, Figure 3A–C. From these results it seems clear that $e^2qQ/h \leq 1.2$ MHz. This value is not inconsistent with the range ~0.8–3.27 MHz found by Aime et al. (1983, 1984, 1988) and Brownlee et al. (1986) for a series of metallocarbonyls, using ^{17}O T_1 measurements and τ_R estimates (in the extreme narrowing limit). e^2qQ/h is clearly much smaller than the ~4.4 MHz values found for free $CO_{(gas)}$ (Richardson, 1960; Lefebvre-Brion et

Table I: $C^{16}O$ Vibrational Stretch Frequencies, Oxygen-17 Isotropic Chemical Shifts, and Carbon-13 Isotropic Chemical Shifts for CO–Heme Proteins and a Model System

sample	$\nu(C-^{16}O)$ (cm^{-1})	ref	$\delta_i(^{17}O)$ (ppm)	$\delta_i(^{13}C)$ (ppm)	ref
G. dibranchiata hemoglobin	1970	*a*	372.7	205.9	
				205.45	*b*
				206.2	*c,d*
synthetic *P. catodon* myoglobin (His E7 → Val), pH = 7.0	1970	*e*	371.7		
picket fence porphyrin	1967	*f*	372	205.4	*g*
synthetic *P. catodon* myoglobin (His E7 → Phe), pH = 7.0	1967	*e*	371.7		
cytochrome P-450_{CAM} (E.C. 1.14.15.1)	1963	*h*		200.3	*i*
hemoglobin Zürich (His E7β → Arg), pH = 7.7	1958	*j*		205.5	*j*
chloroperoxidase (E.C. 1.11.1.10)					
pH = 6.0	1958	*k*	368.6		
pD = 5.8				200.8	*l*
human adult hemoglobin	1951	*j*	369	206.4	*j*
α chain, pH = 7.0				206.75	*m*
				207.5	*c*
β chain, pH = 7.0	1951	*j*	369	206.19	*m*
				207.1	*c*
rabbit hemoglobin, β chain, pH = 7	1951	*a*	369, 370.1	206.4	
				206.3	*a*
				206.18	*m*
P catodon myoglobin					
pH = 7.0	1944	*n*	366.5	208.7	*c*
pH = 7.2				207.93	*b*
pH = "low"	1967	*o*	370.7		
lactoperoxidase (E.C. 1.11.1.7,8)	1941	*p*		208.3	*l*
rabbit hemoglobin, α chain, pH = 7.0	1928	*a*	361, 361.7	208.0	
				208.18	*m*
horseradish peroxidase isoenzyme A (E.C. 1.11.1.7)					
pH = 9.5	1932	*q*	362.6		
pD = 6.8	1923	*q*		208.9	*l*
pH = 4.5	1909	*q*	355.5		
horseradish peroxidase isoenzyme C (E.C. 1.11.1.17)					
pH = 7	1913	*q*	358.4		
pH = 10.5	1932	*q*	365.0		
pD = 6.4	1913	*q*		209.1	*l*

[a] Satterlee et al. (1978). [b] Moon et al. (1977). [c] Perkin et al. (1983). [d] Perkins (1982). [e] This work. [f] Collman et al. (1976). [g] Lee et al. (1988). [h] Uno et al. (1985). [i] N. A. Matwiyoff and S. B. Philson, unpublished results [quoted in Berzinis and Traylor (1979)]; S. Philson, private communication). [j] Choc and Caughey (1981). [k] O'Keefe et al. (1978). [l] Behere et al. (1985). [m] Moon and Richards (1974). [n] Tsubaki et al. (1982). [o] Ramsden and Spiro (1989). [p] Smith et al. (1984). [q] Barlow et al. (1976), Uno et al. (1987), and Evangelista-Kirkup et al. (1986). Values shown are our estimates of the exchange-averaged frequencies with the particular isoenzyme indicated; pH values shown correlate with the NMR chemical shift determinations.

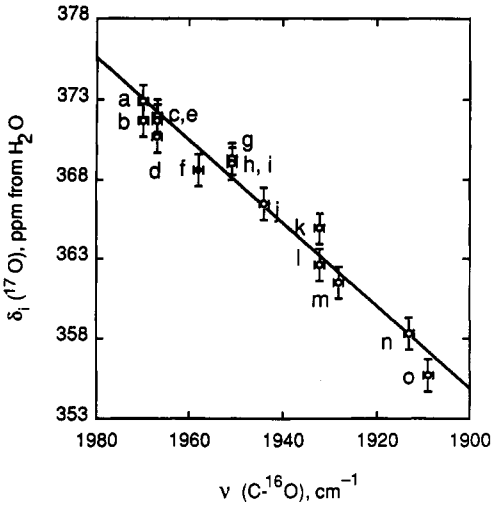

FIGURE 5: Graph showing relation between infrared CO vibrational stretch frequency [ν(C–O), cm^{-1}] and ^{17}O NMR isotropic chemical shift, $\delta_i(^{17}O)$, for heme proteins. Data points for proximal His as well as proximal Cys (chloroperoxidase) fall on the same curve. Letters correspond to proteins, as follows: a, *G. dibranchiata* hemoglobin; b, synthetic *P. catodon* myoglobin His E7 → Val; c, picket fence porphyrin; d, *P. catodon* myoglobin, pH "low"; e, synthetic *P. catodon* myoglobin, His E7 → Phe; f, chloroperoxidase, pH = 6.0; g, rabbit hemoglobin, β chain; h, human adult hemoglobin, α chain; i, human adult hemoglobin, β chain; j, *P. catodon* myoglobin, pH = 7.0; k, horseradish peroxidase isoenzyme C, pH = 10.5; l, horseradish peroxidase isoenzyme A, pH = 9.5; m, rabbit hemoglobin, α chain; n, horseradish peroxidase isoenzyme C, pD = 7.0; o, horseradish isoenzyme A, pD = 4.5.

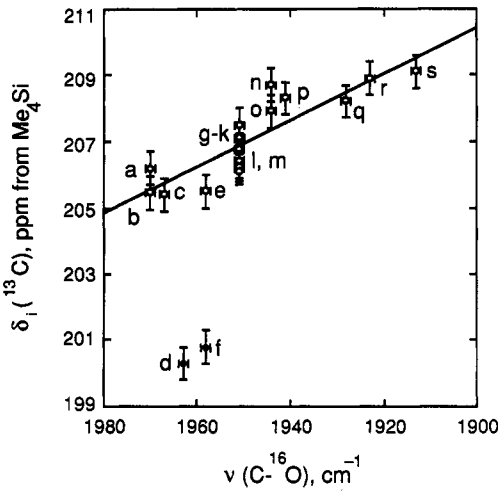

FIGURE 6: Graph showing relation between $\nu(^{12}C–O)$ and carbon-13 NMR isotropic chemical shift (for ^{13}CO ligands) in heme proteins. The upper data points fit fairly closely to a linear relation and are all from proteins containing a proximal His residue, while the two points below the line are from the proximal Cys-coordinated proteins, cytochrome P-450_{CAM} and chloroperoxidase. Data points are as follows: a, *G. dibranchiata* hemoglobin; b, *G. dibranchiata* hemoglobin; c, picket fence porphyrin; d, cytochrome P-450_{CAM}; e, hemoglobin Zürich, pH = 7.7; f, chloroperoxidase, pH = 5.8, g, human adult hemoglobin, α chain; h, human adult hemoglobin, α chain; i, human adult hemoglobin, α chain; j, human adult hemoglobin, β chain; k, human adult hemoglobin, β chain; l, rabbit hemoglobin, β chain; m, rabbit hemoglobin, β chain; n, *P. catodon* myoglobin, pH = 7.0; o, *P. catodon* myoglobin, pH = 7.2; p, lactoperoxidase, pD = 6.8; q, rabbit hemoglobin, α chain; r, horseradish peroxidase isoenzyme A, pD = 6.8; s, horseradish peroxidase isoenzyme C, pD = 6.4.

al., 1963; Lovas & Tiemann, 1974; Amos, 1979; Cummings et al., 1987) or for CO groups in a range of organic compounds (6–12 MHz; Kintzinger, 1981).

While the computer simulation, Figure 3C, of the experimental spectrum, Figure 3D, is not exact, due possibly to the presence of more than one conformational substate, the ~1.2 MHz value of $|e^2qQ/h|$ does appear to be an upper limit, since, e.g., e^2qQ/h = 2.0 MHz generates a noticeably broader line, which in addition has second-order structure visible (seen clearly in the 3 MHz simulation, Figure 3A). Our e^2qQ/h value is thus located at one extreme end of the range found previously for other metallocarbonyls. This is a result that might be expected if back-bonding from Fe d orbitals is the primary cause for the reduction in e^2qQ/h from the ~4.4

MHz value found in free CO. In the picket fence porphyrin, we have only one CO ligand capable of strong π-back-bonding, so there is less competition for the Fe d electrons, i.e., we are seeing basically the operation of a trans influence. Additional (especially trans) strong π-bonding ligands would reduce the amount of back-donation possible, increasing e^2qQ/h. For a more detailed discussion of π-bonding effects the reader is referred to Caughey et al. (1969).

In CO gas itself, the sign of e^2qQ/h has been shown, by microwave experiments, to be positive. The observation that all published e^2qQ/h values for metallocarbonyls are in the range ~1–3 MHz tends to support the idea that these e^2qQ/h values are positive also, since the largest value found (~3.3 MHz) is quite close to that of CO (~+4.4 MHz). None of the published values are less than ~0.8 MHz, so a mixture of signs for the metallocarbonyls seems unlikely. It also seems unlikely that all metallocarbonyls have negative e^2qQ/h values (although it is not impossible), since then we would have no ready explanation for the small e^2qQ/h value found in the picket fence porphyrin, which in our model is due to increased back-donation to the single CO ligand.

We now consider in more detail the ^{17}O chemical shifts in metalloproteins and model systems, and show in Figure 4 ^{17}O solution-state NMR spectra of two mutant $C^{17}O$ sperm whale myoglobins (His E7 → Val; His E7 → Phe), native sperm whale MbCO (pH 7.0 and 4.4), *Glycera dibranchiata* HbCO, rabbit HbCO, and horseradish peroxidase isoenzyme A (pH 9.5 and 4.5). The results on the mutant myoglobins, myoglobin at low pH, and *G. dibranchiata* are new; the results on the other systems are from two previous publications (Lee et al., 1988; Lee & Oldfield, 1989).

Figure 5 shows the observed isotropic ^{17}O NMR chemical shifts plotted as a function of ν(C–O), the infrared CO stretch frequency, for each of the systems investigated, the actual values used being shown in Table I. As noted previously, for the native hemoglobins and myoglobins, there is an excellent correlation between $\delta_i(^{17}O)$ and ν(C–O), with the new data for the mutant myoglobins falling in a region populated by the picket fence porphyrin, *G. dibranchiata* HbCO, and low-pH sperm whale MbCO. In addition, Figure 5 shows that data previously obtained for the high- and low-pH forms of horseradish peroxidase isoenzyme A, as well as for the C isoenzyme and chloroperoxidase, also fall on the same line. Thus, we have our first interesting result that both IR and ^{17}O NMR spectroscopy appear to be reflecting the same type of "fluctuation". Measurement of $\delta_i(^{17}O)$ yields ν(C–O), and vice versa, and the relation can be expressed as

$$\delta_i(^{17}O,\text{ppm}) = 0.2559\nu(\text{C–O})\ (\text{cm}^{-1}) - 131.3 \quad (7)$$

with a correlation coefficient of 0.965.

This result is in rather sharp contrast to that which can be deduced from ^{13}C NMR, as shown in Figure 6. Here again there is a correlation between the observed isotropic chemical shifts, $\delta_i(^{13}C)$, and ν(C–O), as shown previously for a more limited data set by Satterlee (1983), but clearly major deviations from a linear relation are found for chloroperoxidase (which falls on or close to the ^{17}O correlation) and cytochrome P-450_{CAM} (which we have not yet investigated using ^{17}O NMR). Both proteins have proximal cysteine, rather than histidine, coordination and essentially the same ^{13}C chemical shifts (200.8 ppm for chloroperoxidase, 200.3 ppm for cytochrome P-450_{CAM}) (Behere et al., 1985). If both of these cys-coordinated species are eliminated from consideration, we find

$$\delta_i(^{13}C,\text{ppm}) = -0.07041\nu(\text{C–O})\ (\text{cm}^{-1}) + 344.2 \quad (8)$$

with a correlation coefficient of 0.756. The values used to compile Figures 5 and 6 are listed in Table I, together with the relevant literature citations.

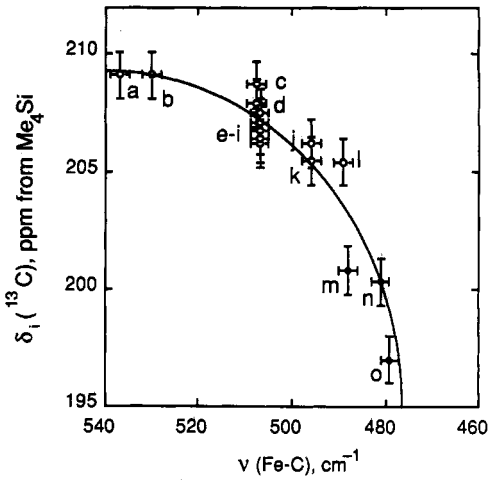

FIGURE 7: Graph showing relation between ν(Fe-C) and $\delta_i(^{13}C)$ for heme proteins and a model heme–thiolate complex. Data from Table II. Points are as follows: a, horseradish peroxidase isoenzyme C, pD = 6.4; b, horseradish peroxidase isoenzyme C; c, *P. catodon* myoglobin, pH = 7.0; d, *P. catodon* myoglobin, pH = 7.2; e, human adult hemoglobin, α chain; f, human adult hemoglobin, α chain; g, human adult hemoglobin, α chain; h, human adult hemoglobin, β chain; i, human adult hemoglobin, β chain; j, *G. dibranchiata* hemoglobin; k, *G. dibranchiata* hemoglobin; l, $Fe^{II}(T_{piv}pp)(NMeIm)CO$; m, chloroperoxidase, pH = 5.8; n, cytochrome P-450_{CAM}, + cam; o, $Fe^{II}T_{piv}pp(C_6HF_4S)CO$.

There are thus several interesting aspects to the ^{13}C and ^{17}O NMR chemical shifts. First, the ^{13}C and ^{17}O shifts are in opposite directions, which cannot reasonably be attributed to a simple change in the ΔE term of the Karplus–Pople equation (Karplus & Pople, 1963)

$$\delta_p^A = \frac{e^2\hbar^2}{2m^2c^2\Delta E}\langle r^{-3}\rangle_{2p}[Q_{AA} + \sum_{B\neq A} Q_{AB}] \quad (9)$$

an effect common in metallocarbonyls, as discussed by Buchner and Schenk (1982). Second, the ^{17}O data correlates well with ν(C–O), while the ^{13}C data does not.

For CO ligands, Buchner and Schenk showed that, for ^{17}O NMR

$$Q_{OO} + Q_{CO} = \tfrac{4}{3}(1 - P^{\sigma}_{z_Oz_C}P^{\pi}_{y_Oy_C}) \quad (10)$$

while for ^{13}C NMR

$$Q_{CC} + Q_{CO} + Q_{CFe} = \tfrac{4}{3}[1 - P^{\sigma}_{z_Cz_O}P^{\pi}_{y_Cy_O} - 3^{1/2}P^{\sigma}_{z_Cz^2_{Fe}}P^{\pi}_{y_Cy_{Fe}}] \quad (11)$$

where $P^{\pi}_{y_Cy_{Fe}}$ is the C–Fe(d_{yz}) π-bond order, $P^{\sigma}_{z_Cz^2_{Fe}}$ is the Fe-(d_{z^2}) σ-bond order, $P^{\sigma}_{z_Cz_O}$ is the C–O σ-bond order, and $P^{\pi}_{y_Cy_O}$ is the C–O π-bond order.

As noted by Buchner and Schenk, as the σ-bond order of $P^{\sigma}_{z_Cz_O}$ is negative, a reduction in the C–O π-bond order ($P^{\pi}_{y_Cy_O}$) results in a smaller value for ($Q_{AA} + Q_{AB}$) in eq 9. A reduction in C–O π-bond order is expected on back-bonding and is predicted to give a smaller paramagnetic shift; i.e., the ^{17}O resonance is shielded upon back-bonding.

For ^{13}C NMR, we must use eq 11, since by virtue of the following bonding scheme

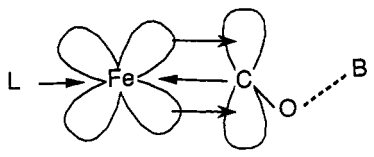

the ^{13}C chemical shift is influenced by both Fe–C and C–O interactions. Using similar arguments, it can be shown that

Table II: Fe–C Vibrational Stretch Frequencies and Carbon-13 Isotropic Chemical Shifts for CO–Heme Proteins and Model Systems

sample	ν(Fe–C) (cm^{-1})	ref	$\delta_i(^{13}C)$ (ppm)
G. dibranchiata hemoglobin	496	*a*	205.45
	496	*a*	206.2
Fe(T_{piv}pp)NMeIm (in benzene)	489	*b*	205.4
cytochrome P-450_{CAM} (E.C. 1.14.15.1)	481 (+camphor)	*c*	200.3
human adult hemoglobin			
α chain, pH = 7.0	507	*d*	206.4
	507	*d*	206.75
	507	*d*	207.5
β chain, pH = 7.0	507	*d*	206.2
	507	*d*	207.1
P. catodon myoglobin			
pH = 7.0	508	*e*	208.7
pH = 7.2	508	*e*	207.9
horseradish peroxidase			
isoenzyme C (E.C. 1.11.1.17), pD = 6.4	530	*f*	209.1
	537	*g*	209.1
chloroperoxidase (E.C. 1.11.1.10)	488	*h*	200.8
heme–thiolate complex (Fe(T_{piv}pp)(C_6HF_4S)(CO))	~479	*i*	197

[a] Carson et al. (1985). [b] Kerr et al. (1983). [c] Uno et al. (1985). [d] Tsubaki et al. (1982). [e] Morikis et al. (1989). [f] Averaged value, Uno et al. (1987). [g] Evangelista-Kirkup et al. (1986). [h] Bangcharoenpaurpong et al. (1986). [i] This value is estimated from a related model heme–thiolate complex: Chottard et al. (1984).

on π-back-donation, the magnitude of $P^{\pi}_{y_C y_{z_{Fe}}}$ increases, resulting in an increased paramagnetic shift (Buchner & Schenk, 1982), basically as noted earlier by Bodner et al. (1973).

Thus, strong back-bonding decreases the C–O π-bond order and decreases the paramagnetic shift for ^{17}O, while simultaneously increasing the Fe–C π-bonding ($P_{y_C}{}^{\pi}{}_{zy_{Fe}}$) and increasing the paramagnetic shift for ^{13}C, assuming that the Fe–C term is larger than the C–O term in eq 11. If this is correct, then we would predict a monotonic relation between ν(Fe–C), which is one monitor of Fe–C back-bonding, and $\delta_i(^{13}C)$, and this relation is indeed found to hold, as shown in Figure 7 and Table II. Of course, ν(Fe–C) reflects both σ and π effects, as indeed does the observed chemical shift. Nevertheless, as can be seen from Figure 7, $\delta_i(^{13}C)$ and ν(Fe–C) for both the His- and Cys-coordinated heme proteins appear to fall on the same curve, in contrast to the rather different behavior seen with the cytochrome P-450_{CAM} and chloroperoxidase ^{13}C NMR data points shown in Figure 6, in which solely the C–O part of the Fe–C–O interaction is reflected [in ν(C–O)].

Presumably, then, there are two main contributions to the ^{13}C chemical shifts: variations in $P^{\pi}_{y_C z y_{Fe}}$ contribute to the general deshielding seen with increased back-bonding among the His-coordinated heme proteins, while increased σ-donation to Fe from the cysteinate ligands in P-450_{CAM} and chloroperoxidases reduces $P^{\sigma}_{z_C z^2{}_{Fe}}$ and causes increased shielding (eq 11). Changes in ΔE on changing the fifth ligand would not be unexpected. However, the observed trends in $\delta_i(^{13}C)$, $\delta_i(^{17}O)$, ν(C–O), and ν(Fe–C) all appear to be consistent with the simple model outlined above. We should also note that there will also likely be a trans influence on $P^{\pi}_{zy_{Fe}y_C}$ due to increased Fe–S back-bonding. Thus, both $P^{\sigma}_{z^2{}_{Fe}z_C}$ and $P^{\pi}_{zy_{Fe}y_C}$ should decrease on replacement of His by the mercaptide ligand—in both instances we expect a shielding effect on $\delta_i(^{13}C)$.

For solely His-coordinated proteins, there is a moderately good correlation between $\delta_i(^{13}C)$ and $\delta_i(^{17}O)$. For the CO heme proteins of interest to us, we might view these effects *very* crudely as an increase of valence form II:

$$\underset{\mathrm{I}}{Fe^{-}-C\equiv O^{+}} \leftrightarrow \underset{\mathrm{II}}{Fe=C=O}$$

with a deshielding of $\delta_i(^{13}C)$ (π-bond formation with Fe) correlating with a shielding of $\delta_i(^{17}O)$ (less π-bond character)—results which of course agree with the ν(Fe–C) and ν(C–O) vibrational frequencies observed by IR and Raman spectroscopy. In particular, the IR and Raman results support the dominance of the Fe–C interaction on ^{13}C chemical shifts since, as can be seen from Figure 7, there is a very large change (~15%) in ν(Fe–C) over the whole range of compounds investigated, while for ν(C–O) there is only a ~3–4% change. If force constant data are used, then this effect is further accentuated. Thus, it appears, on the basis of vibrational data, that Q_{CFe}-like terms will dominate $\delta_i(^{13}C)$, as suggested above. Of course, we should add that we are making here only qualitative statements—since at present there is no satisfactory method of accurately calculating chemical shift tensor elements except in molecules much smaller than heme proteins. It is worth noting, however, that ab initio derivative Hartree–Fock (DHF) calculations on CO accurately predict the ^{13}C and ^{17}O chemical shift tensors for CO (which are known to be very similar to those found in the heme proteins and model system) and also predict quite closely the linear relationships between ^{13}C and ^{17}O shifts and ν(C–O) (Augspurger et al., 1990). Such changes in C–O bond strength could influence the Fe d CO π^*-back-bonding in the manner we suggest in this paper, but further work is necessary in order to accurately model electric fields in heme proteins and to incorporate in an explicit manner bonding to Fe.

Equations 10 and 11 do, however, give a simple chemical explanation of the opposite trends in $\delta_i(^{13}C)$ and $\delta_i(^{17}O)$ found in most metallocarbonyls and our heme proteins, based on the extensive correlations with ν(C–O) and ν(Fe–C).

We now consider briefly what effects a distal residue might have on $\delta_i(^{17}O)$ and $\delta_i(^{13}C)$, for those proteins having His as the fifth ligand. The results shown in Figures 5 and 6 cover a wide range of ^{17}O chemical shifts, 16 ppm, but a much smaller range of ^{13}C chemical shifts, only 3.7 ppm (for His-coordinated systems). The ratio $\delta_i(^{17}O)/\delta_i(^{13}C)$ = 4.3 is considerably larger than the ~1.0 to ~2.4 ratio seen for two series of simple metal carbonyls (Cozak et al., 1979; Gray & Kraihanzel, 1983), in which other ligands were substituted or modified, and is also much larger than the ratio of either the whole chemical shift ranges (~1) or the chemical shift anisotropy (~1.6) found for the group 6 transition-metal carbonyls (Oldfield et al., 1985). We believe these observations suggest that ^{17}O NMR is reporting on changes in the *local* environment of ^{17}O, specifically, on interactions with *distal* residues in the proteins. In the horseradish peroxidases, we and others have noted a pH titration behavior, with $\delta_i(^{17}O)$ becoming more shielded at low pH values. If the distal His is being protonated, as thought by many workers, then clearly form I above would not be favored, and we would anticipate a decrease in ν(C–O), an increase in ν(Fe–C), and a decrease in $\delta_i(^{17}O)$, as is observed experimentally. Similar decreases in ν(C–O) and $\delta_i(^{17}O)$ have been observed in contact ion pairs by Darensbourg and co-workers (Darensbourg et al., 1980, 1982; Darensbourg, 1985; Ash et al., 1986), and Russian workers have observed overall decreases in ν(C–O) in other metal carbonyls on protonation or on hydrogen bond formation (Lokshin et al., 1986, 1988). A simple representation might look like

$$\underset{\mathrm{I}}{Fe^{-}-C\equiv O^{+}} + X^{\delta+} \leftrightarrow \underset{\mathrm{III}}{Fe=C=O^{\delta+}-X} \rightarrow \underset{\mathrm{II}}{Fe=C=O} + X^{\delta+}$$

An increase in ν(Fe–C), a decrease in ν(C–O), and a decrease in $\delta_i(^{17}O)$ might be expected upon interaction with $X^{\delta+}$, which

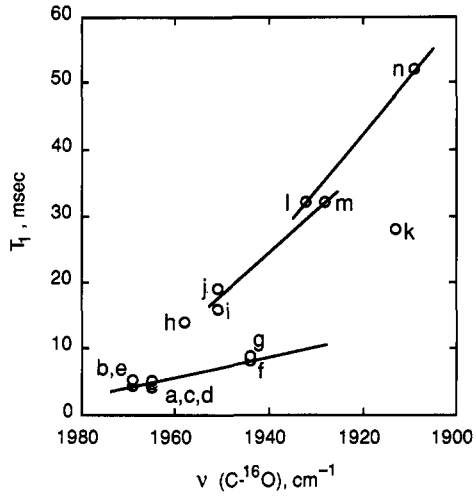

FIGURE 8: Graph showing relation between ν(C–O) and the oxygen-17 spin–lattice relaxation time (T_1). The straight lines join data points for proteins expected to have essentially the same rotational correlation times, τ_R. Data points as follows: a, picket fence porphyrin; b, synthetic *P. catodon* myoglobin, His E7 → Val; c, synthetic *P. catodon* myoglobin, His E7 → Phe; d, *P. catodon* myoglobin, His E7 → Phe; e, *P. catodon* myoglobin, His E7 → Val; f, *P. catodon* myoglobin; g, *P. catodon* myoglobin; h, chloroperoxidase, pH = 6; i, human adult hemoglobin, α and β chains; j, rabbit hemoglobin, β chain; k, horseradish peroxidase isoenzyme C, pH = 7.0; l, horseradish peroxidase isoenzyme A, pH = 9.5; m, rabbit hemoglobin, α chain; n, horseradish peroxidase isoenzyme A, pH = 4.5. Multiple values for a given protein reflect the scatter of isotropic chemical shifts found in the literature.

could be, e.g., a hydrogen bond donor, a charged species such as an imidazolium residue (histidine), or possibly an alkylammonium ion (lysine) or guanidinium residue (arginine) or even a suitably oriented dipole field. In each case, valence form II would be favored. We discuss these possibilities in more depth below.

We now consider the determination of the electric field gradients at oxygen, or, more specifically, we discuss our estimation of the nuclear quadrupole coupling constant, $|e^2qQ/h|$, from spin–lattice relaxation time (T_1) measurements.

We show in Figure 8 and Table III the experimentally observed spin–lattice relaxation times for a range of proteins. We have obtained several new values on native sperm whale myoglobin, together with new results on the His E7 → Val and His E7 → Phe mutants, and will discuss these results together with other previously reported data on rabbit HbCO and horseradish peroxidase, in which we did not determine e^2qQ/h values.

As shown in Figure 8 and Table III, there is a wide range of T_1 values found in heme proteins, varying from 4.3 ms (MbCO His E7 → Val) to 52 ms (horseradish peroxidase isoenzyme A, pH 4.5). As can be seen from the data points in Figure 8, there appears to be some sort of weak relationship between T_1 and ν(C–O), with T_1 in general increasing as ν(C–O) decreases. We suggested above that a decrease in ν(C–O) indicated an increase in back-bonding, with a resultant decrease in C–O π-bond order, and previously we (Oldfield et al., 1985) and others (Aime et al., 1983; Brownlee et al., 1986) suggested that the decrease in e^2qQ/h values found in a variety of metal carbonyls (in the range ~0.8–3 MHz) from the free gas value (~4.4 MHz) was also due, at least in part, to an increase in π-back-bonding. We would thus predict a general decrease in e^2qQ/h as ν(C–O) decreases, which should result in an increase in T_1, outside of the extreme narrowing limit (assuming that this effect is not obscured by τ_R differences).

Because of the range of τ_R values expected for the different molecular weight proteins shown in Figure 8, this relationship

Table III: Oxygen-17 Spin–Lattice Relaxation Times (T_1) for Various CO–Heme Proteins and a Model System and Derived ^{17}O Nuclear Quadrupole Coupling Constants (e^2qQ/h)

system	T_1 (ms)[a]	τ_R (ns)[b]	e^2qQ/h (MHz)[c]
synthetic *P. catodon* myoglobin	4.3	13 ± 3	1.2 ± 0.15
(His E7 → Val)	5.3	13 ± 3	1.1 ± 0.15
picket fence porphyrin	4		(≲1.2)[d]
P. catodon myoglobin	9	13 ± 3	0.84 ± 0.13
	8.3	13 ± 3	0.87 ± 0.13
	8.3	13 ± 3	0.87 ± 0.13
synthetic *P. catodon* myoglobin	4.7	13 ± 3	1.15 ± 0.15
(His E7 → Phe)	5.1	13 ± 3	1.12 ± 0.15
chloroperoxidase, pH = 6	14	20 ± 5	0.86 ± 0.13
human adult hemoglobin, α and β chains	16	30 ± 10	0.96 ± 0.16
rabbit hemoglobin, β chain	19	30 ± 10	0.87 ± 0.17
horseradish peroxidase isoenzyme A, pH = 9.5	32	25 ± 8	0.60 ± 0.11
rabbit myoglobin, α chain	32	30 ± 10	0.67 ± 0.13
horseradish peroxidase isoenzyme C, pH = 7.0	28	25 ± 8	0.66 ± 0.10
horseradish peroxidase isoenzyme A, pH = 4.5	52	25 ± 8	0.47 ± 0.09

[a] Spin–lattice relaxation time, T_1 (ms), as determined from a 180–τ–90 experiment, as described in the text. [b] Rotational correlation time, τ_R (ns), for assumed isotropic rotation, as described in the text. The myoglobin and hemoglobin values have been determined in a number of ways, and the error bars cover most values (at comparable concentrations and temperatures). The τ_R values for the other systems are our estimates, based on size considerations. [c] Quadrupole coupling constant, in megahertz. [d] Value deduced from line-shape simulations of a solid sample, using magic-angle sample spinning, as described in the text.

is not overwhelming when all the data are viewed together. However, if we add lines joining individual data points within the myoglobin, hemoglobin and HRP-A data families (Figure 8), then it becomes more obvious that, *within a particular family*, there is in an increase in T_1 as ν(C–O) decreases. Since τ_R is not expected to change because of the His → Val, Phe mutation or due to a pH change (horseradish peroxidase) or an intersubunit or interspecies comparison (hemoglobins), then the results of Figure 8 do in fact indicate that e^2qQ/h decreases as ν(C–O) decreases, in accord with similar force constant results of Brownlee et al. (1986) on a series of organometallic complexes.

We can determine $|e^2qQ/h|$ from measurements of T_1 much as we did previously (Lee & Oldfield, 1989), using the relationship

$$\frac{1}{T_1} = \frac{3\pi^2}{50}\,\frac{2I+3}{I^2(2I-1)}\left(\frac{e^2qQ}{h}\right)^2\left[\frac{\tau_R}{1+\omega_0^2\tau_R^2}+\frac{4\tau_R}{1+4\omega_0^2\tau_R^2}\right] \quad (12)$$

which is though to be valid in the range $\omega_0\tau_R < 10$ we are working in (Hubbard, 1970; Bull, 1972; Reuben & Luz, 1976; Bull et al., 1979; Halle & Wennerström, 1981; Andersson et al., 1982; Lerner & Torchia, 1986). Here, I is the nuclear spin quantum number for ^{17}O (=$^5/_2$), and ω_0 is the Larmor frequency ($2\pi \times 68 \times 10^6$ rad s^{-1}). Figure 9 shows graphical solutions to eq 12 for T_1 as a function of τ_R and e^2qQ/h.

In order to estimate e^2qQ/h, we used the following τ_R values: for all MbCO's (same concentration, temperature), τ_R = 13 ± 3 ns, as reported previously (Lee & Oldfield, 1989). For all HbCO's, τ_R = 30 ± 10 ns. The range 20–40 ns covers essentially all τ_R values previously determined close to this concentration, pH, and temperature. For the horseradish peroxidases, we estimate τ_R = 25 ± 8 ns, based on its size

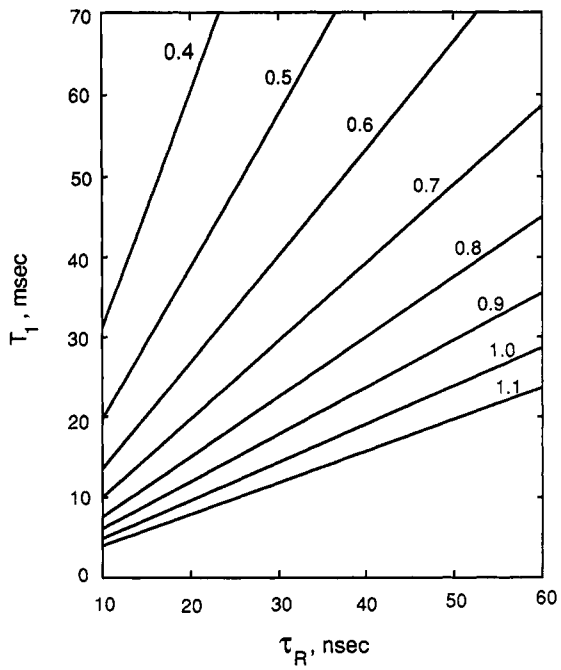

FIGURE 9: Graph showing theoretical relationship between the ^{17}O spin–lattice relaxation time (T_1) and the rotational correlation time (τ_R) as a function of quadrupole coupling constant (e^2qQ/h, shown on each curve in megahertz), for relaxation via the quadrupolar mechanism, outside the "extreme-narrowing" limit ($10 \geq \omega_0\tau_R > 1$).

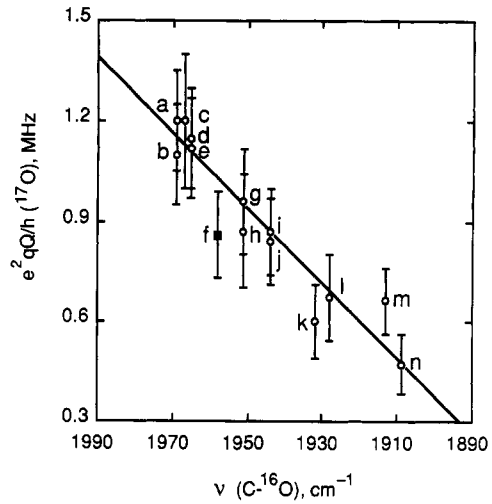

FIGURE 10: Graph showing relation between ν(C–O) and ^{17}O e^2qQ/h for CO-liganded heme proteins. Data points from Table III are as follows: a, synthetic *P. catodon* myoglobin, His E7 → Val; b, synthetic *P. catodon* myoglobin, His E7 → Val; c, picket fence porphyrin; d, synthetic *P. catodon* myoglobin, His E7 → Phe; e, synthetic *P. catodon* myoglobin, His E7 → Phe; f, chloroperoxidase, pH = 6; g, human adult hemoglobin, α and β chains; h, rabbit hemoglobin, β chain; i, *P. catodon* myoglobin; j, *P. catodon* myoglobin; k, horseradish peroxidase isoenzyme A, pH = 9.5; l, rabbit hemoglobin, α chain; m, horseradish peroxidase isoenzyme C, pH = 7.0; n, horseradish peroxidase isoenzyme A, pH = 4.5. Multiple entries for some proteins reflect scatter on individual T_1 determination.

relative to Hb, and we used similar reasoning to estimate τ_R = 20 ± 5 ns for chloroperoxidase. We did not determine τ_R values (as we did previously for MbCO and HbCO) for the peroxidases since uncertainties in the chemical shift anisotropy, and possible exchange broadening, make determination of the residual quadrupolar contribution uncertain.

We show in Figure 10 and Table III the computed e^2qQ/h values as a function of ν(C–O), and in Figure 11 we show these computed e^2qQ/h values as a function of $\delta_i(^{17}O)$. Although there is no a priori reason for either correlation to be linear, there does appear to be a linear relationship between e^2qQ/h and ν(C–O) and between e^2qQ/h and $\delta_i(^{17}O)$. The linear relations between e^2qQ/h and ν(C–O) or between e^2qQ/h and δ_i are not general for ^{17}O NMR of metal carbonyls, as can be seen by inspection of $e^2qQ/h - \delta_i(^{17}O)$ results for 39 different CO ligands in metallocarbonyls (Aime et al., 1983, 1984, 1988; Hawkes et al., 1984). These results show essentially no correlation, although it is interesting to note that there are no $|e^2qQ/h|$ values below ~1.0 MHz. Both heme protein data sets indicate that there is unlikely to be a sign change between any of the systems we have investigated, and we believe that the same is likely to hold true for the other transition-metal carbonyls. Thus, all e^2qQ/h values can be compared with each other. On the basis of the results of ab initio calculations on CO and of experimental results, as discussed earlier, the sign of e^2qQ/h is thought to be positive.

We now have the following two additional relationships for heme proteins:

$$e^2qQ/h\ (\text{MHz}) = 0.01128\nu(\text{C–O})\ (\text{cm}^{-1}) - 21.06 \qquad R^2 = 0.921 \quad (13)$$

and

$$e^2qQ/h\ (\text{MHz}) = 0.04178\delta_i(^{17}O)\ (\text{ppm}) - 14.42 \qquad R^2 = 0.904 \quad (14)$$

Calculation of the δ_i and e^2qQ/h values for CO in heme proteins is expected to be a difficult task. Nevertheless, we have had moderate success in reproducing the observed e^2qQ/h value for free CO (~4.4 MHz) using a Gaussian-88 program (at the 6-31G* level) (Frisch et al., 1988), finding e^2qQ/h = 3.1 MHz. We have also found that hydrogen bonding, in this case to HF, causes a significant *decrease* in e^2qQ/h, with about a 0.7 MHz decrease found for the linear species CO···HF, Figure 12. There could thus be both a direct influence (decrease in e^2qQ/h, due to hydrogen bonding) and a more indirect effect, due to back-bonding, in the heme proteins. Work on computation of CO electric field gradients in the presence of local electric fields using DHF methods is currently in progress.

Structural Information. We now consider the above spectroscopic results in light of data from other spectroscopic and diffraction techniques.

The first general observation we can make is that IR [ν(C–O)] and ^{17}O NMR appear to reflect a common origin in all systems investigated. From Figure 5, we would suggest that this origin is a change in π-back-bonding (C–O bond order) caused by a distal pocket amino acid interaction. The following pieces of information suggest there is a charge field interaction—which could in principle be due to hydrogen bonding, ion–dipole, or possibly dipole–dipole interactions—the actual nature of the interaction varying from one protein to another.

(1) His E7 is highly conserved in both hemoglobins and myoglobins (Antonini & Brunori, 1971; Waterman & Stengal, 1974). However, in elephant Mb (Romero-Herrera et al., 1981) there is a His E7 → Gln substitution. Unlike most His E7 mutations, which in general lead to a large increase in ν(C–O) (presumably due to removal of the His side chain from close proximity to CO), in elephant MbCO ν(C–O) actually *decreases* from the "normal" value found in sperm whale (~1944 cm^{-1}) to 1937 cm^{-1} (Kerr et al., 1985). Similar results are reported for elephant MbO_2 versus sperm whale MbO_2. While these authors do suggest that their analysis of the vibrational frequencies indicates that the Fe–C–O unit becomes more bent, they also suggest that the interactions of bound O_2 are not markedly affected by the glutamine replacement

and go further to suggest that hydrogen bonding of the amide hydrogen and the CO oxygen could also occur and could be responsible for the enhanced CO binding in elephant MbCO.

One possible explanation of both of the above observations is that *both* O_2 and CO can hydrogen bond to some distal residues. This would not be wholly unreasonable, since, as shown below, histidine and glutamine have similar side-chain structures, from CO to N^{ϵ}:

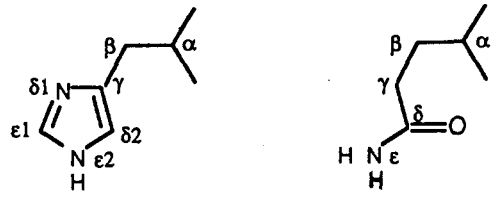

IV V

That is to say, the structure of glutamine can be fairly closely mapped onto that of histidine; the molecular volumes of the whole side chains are very similar (His, 91.9 mL mol^{-1}; Gln, 86.3 mL mol^{-1}; Zamyatnin, 1972), and there is a nitrogen at the ϵ position of both side chains. Given that there are functional roles for the distal residue in normal myoglobins and hemoglobins (Perutz, 1989), it seems plausible to suppose that the following types of resonance stabilization might occur, for oxy proteins:

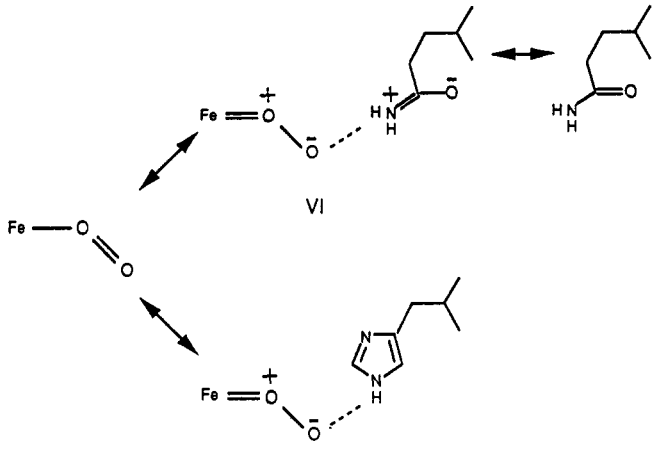

VI

VII

Both VI and VII could be stabilized due to a charge field or hydrogen bond interactions with the bound O_2. The "anomalously" low ν(C–O) in elephant MbCO, suggested as one possibility by Kerr et al. (1985), is simply a stabilization of structure II noted above, as follows:

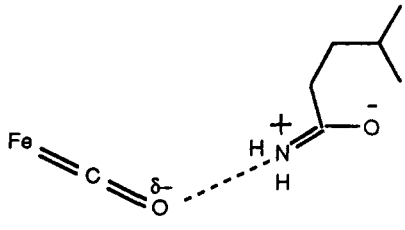

VIII

Notably, removal of the distal His by mutation (our His E7 → Val, Phe mutants) causes a very large (~15–21 cm^{-1}) increase in ν(C–O). If the low ν(C–O) due to E7 His → Gln in elephant myoglobin is due in part to hydrogen bonding, then a similar interaction, albeit weaker, could occur for the histidine residue—a point we return to below. The other pos-

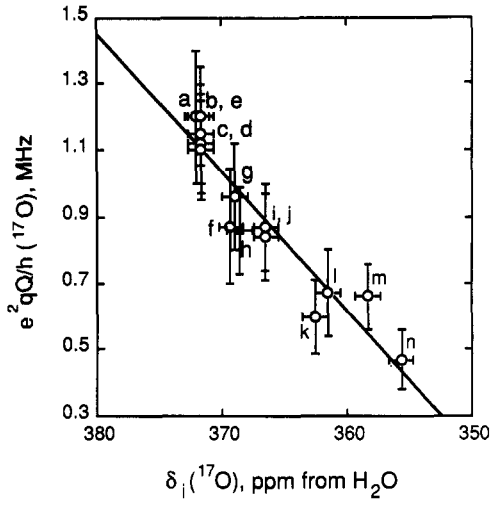

FIGURE 11: Graph showing relation between δ_i(^{17}O) and e^2qQ/h(^{17}O) for C^{17}O-labeled heme proteins. Data points are as follows: a, picket fence porphyrin; b, synthetic *P. catodon* myoblobin, His E7 → Val; c, synthetic *P. catodon* myoglobin, His E7 → Phe; d, synthetic *P. catodon* myoglobin, His E7 → Phe; e, synthetic *P. catodon* myoglobin, His E7 → Val; f, rabbit hemoglobin, β chain; g, human adult hemoglobin, α and β chains; h, chloroperoxidase, pH = 6; i, *P. catodon* myoglobin; j, *P. catodon* myoglobin; k, horseradish peroxidase isoenzyme A, pH = 9.5; l, rabbit hemoglobin α chain; m, horseradish isoenzyme C, pH = 7.0; n, horseradish peroxidase isoenzyme A, pH = 4.5.

sibility, of amide oxygen interaction with the ligand carbon, is basically analogous to the nucleophilic attack model of Maxwell and Caughey (1976) quoted by Fuchsman and Appleby (1979) in their work on MbCO. However, Ramsden and Spiro have recently pointed out that "Such an interaction is unlikely, however, since it would weaken the Fe–C as well as the CO bond...", which is not what is seen experimentally in a variety of systems (Ramsden & Spiro, 1989). For elephant MbCO also, ν(Fe–C) *increases*, from 512 to 515 cm^{-1}, upon the substitution His E7 → Gln (Kerr et al., 1985), and the unreported ^{13}C δ_i appears further downfield than in mammalian hemoglobin [G. LaMar, unpublished results; quoted in Satterlee (1983)]—indicating as Satterlee has noted that "there seem to be better distal ligands...than histidine E7".

(2) In opossum hemoglobin, there is also the substitution His E7α → Gln (Romero-Herrera et al., 1981). Moon et al. (1977) have reported ^{13}C NMR spectra of the α chain of opossum HbCO and find δ_i = 207.42 ppm. For most species, δ_i^{13}C(α) is at 206.7 ppm. By use of the various relations described before, this would correspond to a ~10-cm^{-1} decrease in ν(C–O) for the conversion His E7 → Gln, quite close to the 7 cm^{-1} found for elephant MbCO.

(3) Nagai et al. (1987) have recently reported numerous studies on a wide variety of hemoglobin mutants prepared by site-directed mutagenesis. For a His E7β → Gln mutant, their 2.12-Å resolution difference Fourier map of oxyhemoglobin implies Gln E7β is well localized and "can probably donate a hydrogen bond to the oxygen molecule with better geometry...since the Gln side chain is more flexible than the His side chain". For the Gln E7β mutant, ν(C–O) was found to be *identical* (1951 cm^{-1}) with that of the normal adult hemoglobin (His E7β) and Nagai et al. note that "...Although a neutron diffraction study of CO–Mb showed no hydrogen bond between CO and the distal His E7...polarities of the E7β residue affected the nature of the Fe–CO bond".

(4) Removal of His E7 and replacement with a nonpolar amino acid residue, either by site-directed mutagenesis in sperm whale myoglobin (this work) or by interspecies comparison (e.g., in *G. dibranchiata*), results in a large increase

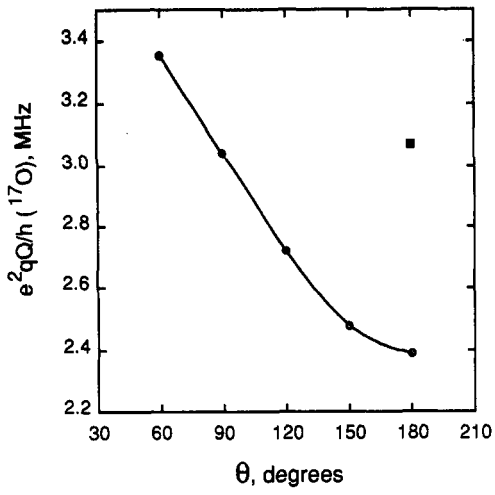

FIGURE 12: Graph of computed e^2qQ/h for oxygen-17 in a CO molecule (r_{CO} = 1.114 Å) interacting with an HF (r_{HF} = 0.911 Å) molecule (CO···HF), having $r_{H\cdots O}$ = 2.149 Å, as a function angle, θ, between the molecular axes, computed by using a Gaussian-88 program at the 6-31G* basis set level.

in ν(C–O) and $\delta_i(^{17}O)$ and a decrease in $\delta_i(^{13}C)$. The ν(C–O) and $\delta_i(^{17}O)$ values for the His E7 → Val and Phe myoglobin mutants are given in Table I, as are the ^{13}C and ^{17}O chemical shifts of *G. dibranchiata* hemoglobin (a possibly heterogeneous mixture but containing primarily Leu E7). We find for the myoglobin mutants ν(C–O) = 1970 cm^{-1} (Leu), 1970 cm^{-1} (Val), and 1967 cm^{-1} (Phe). Nagai et al. find in a His E7β → Val hemoglobin mutant that ν(C–O) = 1971 cm^{-1}, and for a His E7β → Gly mutant, ν(C–O) = 1971 cm^{-1} also. Thus, all His E7 mutations yielding nonpolar amino acids give essentially the same ν(C–O) ($\approx$1969 cm^{-1}), the value expected for a model protoheme in benzene (Caughey, 1980). The large decrease in ν(C–O) and $\delta_i(^{17}O)$ and increase in $\delta_i(^{13}C)$ in the mutants is thus attributable solely to removal of the distal histidine residue and is caused primarily by back-bonding changes due to interactions with the charge field of the E7 side chain.

(5) We now discuss pH effects. Increasing the positive charge on the distal residue is expected to cause increased back-bonding due to stabilization of structures such as II, IX, etc.

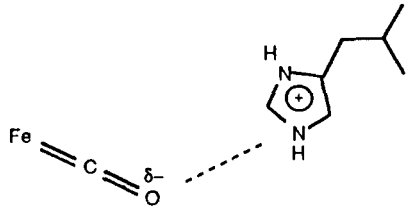

IX

In the peroxidases, e.g., horseradish peroxidase isoenzyme A, it is thought that there is a distal histidine residue that titrates with a pK_a = 6.7 (Barlow et al., 1976). In the case of HRP-A, we find that protonation causes a large ^{17}O NMR shielding and a considerable decrease in e^2qQ/h, consistent with the π-back-bonding picture (Evangelista-Kirkup et al., 1986), in this case due to an increased charge on the distal histidine and increased likelihood of back-donation and/or hydrogen-bond formation or protonation. In the Raman, ν(Fe–C) increases and as expected ν(C–O) decreases, consistent with the ^{17}O NMR results and the observation of a highly deshielded (Fe=C=O) horseradish peroxidase $\delta_i(^{13}C)$ = 209.1 ppm, at pH = 6.8 (Behere et al., 1985).

There are several other pH effects of interest, which fit in with the π-back-bonding/charge field idea, as well as with results on other mutants, to be discussed later.

In horseradish peroxidase isoenzyme C, there is an acid–base transition, this time in the region of p$K_a \approx$ 10.5. Possible candidates for the distal amino acid are tyrosine (pK_a = 10.9) or lysine (pK_a = 10.8), and while we cannot differentiate between them on the basis of our NMR measurements, lysine would be more consistent with our previous discussions, since it has one more formal charge than tyrosine, in either the acidic or basic form. In any case, both the high- and low-pH forms of the A and C isoenzymes of horseradish peroxidase fall on the $\delta_i(^{17}O)$–ν(C–O), e^2qQ/h–ν(C–O), e^2qQ/h–$\delta_i(^{17}O)$, and $\delta_i(^{13}C)$–ν(Fe–C) curves shown previously; so again it seems that only a single interaction is dominating the vibrational frequencies, chemical shifts, and electric field gradients.

We should also note that the *opposite* type of shift *can* be induced on protonation, as in the case of sperm whale MbCO. However, this represents the trivial effect of removal of the distal His from close proximity to the CO ligand, as suggested in a recent Raman study by Ramsden and Spiro (1989) and Morikis et al. (1989). These authors concluded that ν(C–O) in the low-pH limit would be at ~1967 cm^{-1}. We also find, via ^{17}O NMR, that sperm whale MbCO titrates in the low-pH region (Figure 13), and our result indicates a 370.7-ppm low-pH value, essentially the same as that found for the His E7 → Val, Phe MbCO mutants (Table I), at 371.7 ppm, confirming the idea that His is prevented from interacting with the CO ligand by moving out of the heme pocket. Basically the same conclusion can be drawn from previous ^{13}C NMR studies. Thus, we can use the early ^{13}C chemical shifts of sperm whale MbCO, in the pH range 6.79–7.49 (–14.89 ppm from CS_2; Moon & Richards, 1972) and at pH = 5.42 (–14.61 ppm from CS_2; Moon & Richards, 1972) to conclude, using the relationships we have outlined above, that this corresponds to a ~+3.12 cm^{-1} increase in ν_{CO}, at pH = 5.42. From the suggested pK_a of ~4.4 (Wilbur & Allerhand, 1977; Fuchsman & Appleby, 1979; Ramsden & Spiro, 1989), this corresponds to a low-pH-limiting ν(C–O) of $\approx$1975 cm^{-1}, close to that deduced from the Raman data (Morikis et al., 1989). A similar calculation of the oxygen-17 shift from the carbon-13 data yields $\delta_i(^{17}O,H^+)$ ~376 ppm, in the general region expected for no distal charge field interaction.

We note here that the Raman workers (Ramsden & Spiro, 1989) found a pK_a of 4.3, rather than 4.6 calculated by Fuchsman and Appleby (1979), and choose to use the average, 4.4, as the pK_a of the distal histidine. They "choose 4.4 as the best value since it corresponds to the pK_a of what is likely to be the distal histidine...as reported by Wilbur and Allerhand" (1977). Now, while the Wilbur and Allerhand study did indeed conclude that the pK_a of the distal His was 4.4, (a) they were investigating MbCN, not MbCO, and (b) they found that the H^{ϵ_2} tautomer was the abundant species, not the H^{δ_1} form, which is thought to be the major tautomer in crystalline MbCO (Norvell et al., 1975; Hanson & Schoenborn, 1981; Cheng & Schoenborn, 1990). We believe a possible explanation of the apparently identical pK_a of the distal His in MbCO and MbCN in that they are in fact the same, and both, in aqueous solution, are present as the conventional H^{ϵ_2} tautomer and are hydrogen bonded to the axial ligand. In the crystalline solid, things appear to be different, with the unconventional H^{δ_1} tautomer the predominant species. While somewhat speculative, it may be possible to clarify the vexing question of the presence of a hydrogen bond in solution, at least to the extent of determining which tautomer is present in MbCO, via ^{13}C NMR of MbCO (and suitable mutants), using

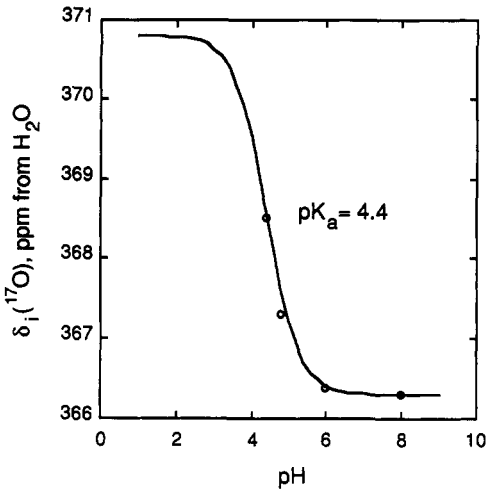

FIGURE 13: Graph showing titration behavior of the $C^{17}O$ ligand in *P. catodon* myoglobin. The circles represent experimental determinations of $\delta_i(^{17}O)$ as a function of pH. The solid line is a Henderson–Hasselbach curve constructed by using a pK_a = 4.4 and a δ_i (high-pH limit) = 366.3 ppm.

the Wilbur and Allerhand approach. Work is in progress in this area, but the results may still not be very definitive because of the change in local environment caused upon His E7 protonation (i.e., it appears to move out of the heme pocket). We should also note that ^1H NMR studies do not "see" either H^{δ_1} or H^{ϵ_2}, due to exchange (P. E. Wright and T. Pochapsky, private communication), although His E7 appears to be oriented in a manner consistent with an H^{ϵ_2}---OC hydrogen bond (or other weak interaction), in aqueous solution (T. Pochapsky, private communication).

(6) Other charge field mutants. One human mutation of particular interest, since it involves a charged residue (E7(63)β Arg), is that found in hemoglobin Zürich (Perutz & Lehmann, 1968), which has been investigated by both ^{13}C NMR and vibrational spectroscopy, as well as by X-ray diffraction (Tucker et al., 1978; Choc & Caughey, 1981). The IR data show ν(C–O) increases from 1951 → 1958 cm^{-1} (with small shoulders for the β subunit at 1968 and 1951 cm^{-1}). The population-weighted average is 1957 cm^{-1}. From the ^{13}C NMR study, we find that there is a 0.5 ppm shielding on conversion from His E7(63)β → Arg, which would translate to a 2.3-ppm ^{17}O deshielding, or a 6-cm^{-1} increase in ν(C–O), to the 1957 cm^{-1} actually calculated for the fast-exchange average.

These shifts or vibrational frequencies are quite close to the "unperturbed" values of 1951 cm^{-1} or ~206 ppm found in normal hemoglobins and are quite unlike the values of ~1970 cm^{-1} found for the various mutants or species having nonpolar residues at E7(63)β. We believe that there is, once again, the possibility of a weak interaction between the distal arginine residue and CO, which is responsible for the observed ν(C–O) of 1957 cm^{-1}. It is again interesting to note that the structure of the arginine side chain bears some relation to that of histidine

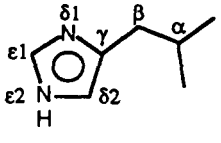

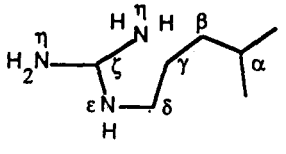

although in the X-ray study the arginine side chain is extended and hydrogen bonds to a heme propionate (Tucker et al., 1978) (note, however, that the reported X-ray structure is for met-Mb, not the CO form). The structure was not, however, refined to detect the three conformers indicated from the IR result, and NMR of course sees a time average. While again quite speculative, it is possible that the 1951-cm^{-1} form represents a normal hydrogen-bonded form, as in the glutamine mutants and species, the 1968-cm^{-1} form represents an arginine completely out of the heme pocket, and the 1958-cm^{-1} form represents the major propionate salt bridge form, with the guanidinium charge having an influence on both ν(C–O) and $\delta_i(^{13}C)$.

(7) Functional evidence for bonding. By suggesting that the distal histidine 64 in native sperm whale myoglobin can interact with the heme-bound carbon monoxide, we look for functional evidence for bonding. The CO dissociation rate constants and equilibrium association constants of the Mb mutants and *G. dibranchiata* have been determined, and are shown in Table IV (Springer et al., 1989; Parkhurst et al., 1980; Seamonds et al., 1976).

In the absence of steric constraints, CO prefers to bind to heme compounds perpendicular to the heme plane (Collman et al., 1976). However, in sperm whale MbCO, carbon monoxide is sterically hindered by the distal histidine 64 to bind in a bent configuration in a densely crowded heme pocket (Stryer, 1988; Caughey et al., 1969a,b). Table IV shows that the Mb mutants have a higher association for CO. This implies that the Mb mutants have allowed CO to adopt a more favorable heme-bound orientation. ^1H two-dimensional NMR studies of the synthetic *P. catodon* His E7 → Phe and His E7 → Val Mb mutants have shown that the respective position 64 residues are in the heme pocket (M. L. Chiu and S. G. Sligar, unpublished results). Since the volume of the valine residue is less than that of histidine, one expects that the CO is allowed to bind in a more perpendicular fashion. However, this argument does not explain the nature of the association of CO to the His E7 → Phe Mb mutant. Although the phenylalanine residue occupies more volume than histidine, CO binds to the His E7 → Phe Mb mutant with a higher affinity than native Mb. Hence, additional mechanisms need to be invoked to explain the CO equilibrium association constant differences.

Low-temperature IR studies of the His E7 → Phe and His E7 → Val MbCO complexes have shown that these mutants have single A states, where an A state corresponds to a bound CO conformation (D. Braunstein and H. Frauenfelder, unpublished results). The multiplicity of the A states in native Mb arises from the polarity, or electric field, of the His E7 residue (Oldfield et al., 1990). In addition, the angle of the CO dipoles from the heme normal of the Phe E7 and Val E7 mutant Mbs align similarly to that of native Mb, as shown in Table IV.

These results imply that the orientations of the CO ligands are similar for the native and synthetic mutant Mbs. However, the mutant synthetic Mbs have higher CO dissociation rate constants than that of native Mb, as shown in Table IV. If the CO is bound in a similar orientation, then hydrogen bond (electric field) stabilization of the CO ligand in native Mb could decrease the dissociation rate.

We should also note that there is a major piece of information that conflicts with any notion of a hydrogen bond interaction, although not with the more general charge field (charge, electric field, or electric field gradient) idea. Specifically, neutron diffraction does not "see" a deuteron at N^{ϵ_2} in MbCO (Norvell et al., 1975; Hanson & Schoenborn, 1981; X. Cheng and B. P. Schoenborn, private communication), while one is visualized at N^{δ_1} (X. Cheng and B. P. Schoenborn, private communication). There is an H bond between H^{ϵ_2} and O_2 in MbO_2, however (Phillips & Schoenborn, 1981). There

Table IV: Thermodynamic Parameters for CO Binding to Sperm Whale Myoglobin and CO–Dipole Tilt Angles from the Heme Normal

system[a]	K_a ($\times 10^{-6}$, M^{-1})[b]	k (s^{-1})[c]	θ (deg)[d]
P. catodon MbCO	29	0.019	15 ± 10, 28 ± 3,[e] 33 ± 4
His 64 → Phe MbCO	83	0.054	21 ± 2
His 64 → Val MbCO	150	0.048	26 ± 3
G. dibranchiata	909[f]	0.042, 0.055[g]	

[a] 5–10 μM protein in 0.1 M phosphate buffer, pH = 7.0, 20 °C. [b] CO equilibrium association constant. [c] CO dissociation rate constant. [d] CO–dipole tilt from the heme normal. [e] Major species. Data from Springer et al. (1989), D. Braunstein and H. Frauenfelder, unpublished results, and Braunstein et al. (1988). [f] Seamonds et al. (1976). [g] Dissociation rate constants for monomeric Hb fractions I and II, 50 mM phosphate buffer, pH 7.0, 20 °C (Parkhurst et al., 1980).

are several possible causes for the lack of observation of a deuteron, apart from the trivial one. Most importantly the crystal, frozen solution, and solution IR spectra of MbCO are all rather different, so it is not easy to correlate the data sets—especially since the IR spectrum of the crystals used for the neutron work is not available. Since the amounts of deoxy- and met-Mb affect the various ν(C–O) values observed, in a crystalline sample of sperm whale MbCO, and since refinements of the MbCO structure show rather high thermal factors for the histidine, direct comparisons between the results obtained by using different techniques are difficult. Nevertheless, the observation is that there is no deuteron at N^{ϵ_2} seen in the neutron study of MbCO, while one is present in MbO_2. This indicates that it is N^{δ_1} that is protonated in MbCO; that is to say, it is the rare H^{δ_1} tautomer that predominates, presumably being stabilized in this uncommon form by interaction with a nearby residue (or residues). It is not necessarily true that this tautomer would predominate in solution. It would also seem surprising, though not impossible, that the unusually low pK_a of ~4.4 (± 0.1) of the H^{ϵ_2} tautomer (in MbCN; Wilbur & Allerhand, 1977) would be the same as that of the H^{δ_1} form in MbCO (Ramsden & Spiro, 1989).

On the other hand, all of the $\delta_i(^{17}O)$, $\delta_i(^{13}C)$, e^2qQ/h, ν(C–O), and ν(Fe–C) data tend to support a picture in which distal polar residues (His, Gln, Lys, and Arg) interact with bound CO ligands, and the shifts and electric field gradients in several instances can be correlated with hydrogen bond or local charge field interactions (e.g., Arg in Hb Zürich). Overall, our picture is thus very similar to that of Li and Spiro (1988), in which they conclude that any effects of Fe–CO distortion on the vibrational frequencies are due to back-bonding changes, which we believe dominate the NMR data. The general conclusion of a number of workers is that there is some sort of a "polarity effect" between CO and the distal histidine (or glutamine) residue, and the neutron study (Hanson & Schoenborn, 1981) does conclude that the N^{ϵ_2}–O distance (2.7 Å) in MbCO is shorter than that expected for a nonbonded N···O interaction. We feel that carbonyl···amide or imidazole hydrogen-bonding or electric field interactions in many of these systems, in solution, would be a suitable description of these polar interactions. Further theoretical work, using techniques developed on simpler molecules (Dykstra, 1988), will hopefully help to clarify some of these ideas, by direct calculation of the relevant observables by using realistic molecular models of the distal charge distributions, and, as noted above, good progress with free CO–charge/electric field/electric field gradient interactions has already been made (Augspurger et al., 1990).

Finally, we consider the actual magnitude of the chemical shift anisotropy of ^{13}CO bound to a heme protein, which should also be a probe of heme–ligand interactions. For many metal carbonyls, and CO itself, the ^{13}C chemical shift anisotropy, $\Delta\delta$, is ~400 ppm (Oldfield et al., 1985). However, for ^{13}CO–hemoglobin, HbCOA, Perkins et al. (1983) have reported the much smaller value of $\Delta\delta$ = 198 ppm. We have determined the ^{13}C T_1 and T_2 values for sperm whale MbCO under similar solution conditions to those used for our isotropic shift measurements and find T_1 = 372 ms and T_2 = 5.8 ms (with 5–10% error limits on both measurements). Assuming τ_R = 13 ns, we find solutions to the relaxation equations having $\Delta\delta$ = 500 ppm and $\langle r_{CH} \rangle$ = 1.8 Å (the latter value being essentially the same as that determined by Perkins et al. for HbCOA). Our value of $\Delta\delta$ is 25% larger than that found for most other metallocarbonyls but is not inconsistent with the larger ^{17}O CSA found in the picket fence porphyrin ($\Delta\delta$ = 814 ppm). In fact, if we use the observation that the ^{17}O CSA in the group 6 metallocarbonyls is, on average, ~1.614 times larger than the ^{13}C CSA (Oldfield et al., 1985), we arrive at a "predicted" ^{13}C CSA for the picket fence porphyrin of ~814/1.614 = 504 ppm, very close to the value determined for MbCO (perhaps by coincidence). In any case, the ^{13}C CSA value of $\Delta\delta$ = 500 ppm is the only solution found from our high-field ^{13}C relaxation measurements, is approximately that which might be expected on the basis of previous ^{13}C and ^{17}O shift tensor results, and is ~2.5 times larger than previous results on HbCOA (Perkins et al., 1983).

Postscript. After completion of this work, we finalized development of an electrical model for distal ligand interactions that puts on a more quantitative basis many of the qualitative ideas described above, and in addition gives a very simple explanation for the observation of numerous (A_0–A_3, I–IV) substates in the hemoglobins, myoglobins, peroxidases, and leghemoglobin (Augspurger et al., 1990; Oldfield et al., 1990). In this model, we attribute the IR vibrational frequency shifts of CO in different proteins to the interaction of the CO dipole moment, and polarizabilities, with electric fields, and this same electric field influence has also been shown to account in a quantitative manner for the ^{13}C and ^{17}O δ_i shifts, an interaction mediated in this case via the shielding polarizability (Buckingham, 1960; Augspurger et al., 1990; Oldfield et al., 1990).

This approach fits in a very natural way with the more conventional "back-bonding" explanation, as follows: weak electrical interactions originate from the electrostatic field around CO—in many cases this being primarily due to the electric field of the distal histidine (there are four possible fields from the two C^β–C^γ ring-flip isomers of the $H^{\delta_1}/H^{\epsilon_2}$ tautomers of His, giving rise to four "substates"), together with a more global field term arising from the total charge distribution, which will vary from protein to protein. These total electric fields modify the charge distribution in CO, which *then* modulates the degree of back-bonding possible. Thus, back-bonding changes are *caused* by changes in local electrostatic potentials, which in the case of the four major substates seen in many CO heme proteins originate in the four "conformations" possible for a distal histidine residue (Oldfield et al., 1990). If this idea is correct, it adds an important new aspect to our IR and NMR studies—that it should be possible to compute ν_{CO}, $\delta_i(^{13}C)$, $\delta_i(^{17}O)$, and $e^2qQ/h(^{17}O)$ values in heme proteins by incorporating in an explicit manner the electric fields at CO due to the total charge distribution in the protein. There is no conflict with the back-bonding model; rather, the (calculable) electrostatic fields from the protein simply appear to be the *origin* of the changes in back-bonding.

ACKNOWLEDGMENTS

We thank Professors H. Frauenfelder, T. Pochapsky, D. Morikis, C. E. Dykstra, and T. Spiro and Drs. H. C. Lee and

P. E. Wright for helpful comments and Mr. D. Braunstein for IR measurements on carbonylated myoglobins.

Registry No. Fe, 7439-89-6; His, 71-00-1; Gln, 56-85-9; Arg, 74-79-3; Lys, 56-87-1; Cys, 52-90-4; [5,10,15,20-tetrakis(α,α,α,α-*o*-pivalamidophenyl)porphyrinato]carbonyliron(II), 97233-16-4.

References

Aime, S., Gobetto, R., Osella, D., Milone, L., Hawkes, G. E., & Randall, E. W. (1983) *J. Chem. Soc., Chem. Commun.* 794.

Aime, S., Gobetto, R., & Osella, D. (1984) *J. Chem. Soc., Dalton Trans.* 1863.

Aime, S., Botta, M., Gobetto, R., & Osella, D. (1988) *J. Chem. Soc., Dalton Trans.* 791.

Alben, J. O., Beece, D., Bowne, S. F., Doster, W., Eisenstein, L., Frauenfelder, H., Good, D., McDonald, J. D., Marden, M. C., Moh, P. P., Reinisch, L., Reynolds, A. H., Shyamsunder, E., & Yue, K. T. (1982) *Proc. Natl. Acad. Sci. U.S.A. 79*, 3744.

Amos, R. D. (1979) *Chem. Pys. Lett. 68*, 536.

Andersson, T., Drakenberg, T., Forsén, S., Thulin, E., & Swärd, M. (1982) *J. Am. Chem. Soc. 104*, 576.

Antonini, E., & Brunori, M. (1971) in *Hemoglobin and Myoglobin in Their Reactions with Ligands*, Elsevier/North-Holland, Amsterdam.

Anzenbacher, P., Evangelista-Kirkup, R., Schenkman, J., & Spiro, T. (1989) *Inorg. Chem. 28*, 4491.

Ash, C. E., Delord, T., Simmons, D., & Darensbourg, M. Y. (1986) *Organametallics 5*, 17.

Augspurger, J., Dykstra, C. E., & Oldfield, E. (1990) *J. Am. Chem. Soc.* (in press).

Baltzer, L. (1987) *J. Am. Chem. Soc. 109*, 3479.

Baltzer, L., Becker, E. D., Tschudin, R. G., & Gansow, O. A. (1985) *J. Chem. Soc., Chem. Commun.*, 1040.

Bangcharoenpaurpong, O., Champion, P. M., Hall, K. S., & Hager, L. P. (1986) *Biochemistry 25*, 2374.

Barlow, C. H., Ohlsson, P.-I., & Paul, K.-G. (1976) *Biochemistry 15*, 2225.

Behere, D. V., Gonzalez-Vergara, E., & Goff, H. M. (1985) *Biochem. Biophys. Res. Commun. 131*, 607.

Berzinis, A. P., & Traylor, T. G. (1979) *Biochem. Biophys. Res. Commun. 87*, 229.

Bodner, G. M., Kahl, S. B., Bork, K., Storhoff, B. N., Wuller, J. E., & Todd, L. J. (1973) *Inorg. Chem. 12*, 1071.

Braunstein, D., Ansari, A., Berendzen, J., Cowen, B. R., Egeberg, K. D., Frauenfelder, H., Hong, M. K., Ormos, P., Sauke, T. B., Scholl, R., Schulte, A., Sligar, S. G., Springer, B. A., Steinbach, P. J., & Young, R. D. (1988) *Proc. Natl. Acad. Sci. U.S.A. 85*, 8497.

Brownlee, R. T. C., Maxwell, J. O., Shehan, B. P., & Wedd, A. G. (1986) *Aust. J. Chem. 39*, 931.

Buchner, W., & Schenk, W. A. (1982) *J. Magn. Reson. 48*, 148.

Buckingham, A. D. (1960) *Can. J. Chem. 38*, 300.

Bull, T. E. (1972) *J. Magn. Reson. 8*, 344.

Bull, T. E., Forsen, S., & Turner, D. L. (1979) *J. Chem. Phys. 70*, 3106.

Carson, S. D., Constantinidis, I., Satterlee, J. D., Ondrias, M. R. (1985) *J. Biol. Chem. 260*, 8741.

Case, D. A., & Karplus, M. (1978) *J. Mol. Biol. 123*, 697.

Case, D. A., Huynh, B. H., & Karplus, M. (1979) *J. Am. Chem. Soc. 101*, 4433.

Caughey, W. S. (1980) in *Methods for Determining Metal Ion Environment in Proteins: Structure and Function of Metalloproteins* (Darnall, D. W., & Wilkin, R. G., Eds.) pp 95–115, Elsevier/North-Holland, New York.

Caughey, W. S., Eberspaecher, H., Fuchsman, W. H., McCoy, S., & Alben, J. O. (1969a) *Ann. N.Y. Acad. Sci. 153*, 722.

Caughey, W. S., Alben, J. O., McCoy, S., Boyer, S. H., Charache, S., & Hathaway, P. (1969b) *Biochemistry 8*, 59.

Caughey, W. S., Shimada, H., Choc, M. G., & Tucker, M. P. (1981) *Proc. Natl. Acad. Sci. U.S.A. 78*, 2903.

Choc, M. G., & Caughey, W. S. (1981) *J. Biol. Chem. 256*, 1831.

Chottard, G., Schappacher, M., Ricard, L., & Weiss, R. (1984) *Inorg. Chem. 23*, 4557.

Collman, J. P., Brauman, J. I., Halbert, T. R., & Suslick, K. S. (1976) *Proc. Natl. Acad. Sci. U.S.A. 73*, 3333.

Cozak, D., Butler, I. S., & Hickey, J. P. (1979) *J. Magn. Reson. 33*, 149.

Cummins, P. L., Bacskay, G. B., & Hush, N. S. (1987) *J. Chem. Phys. 87*, 416.

Darensbourg, M. Y. (1985) *Prog. Inorg. Chem. 33*, 221.

Darensbourg, M. Y., Jimenez, P., & Sackett, J. R. (1980) *J. Organomet. Chem. 202*, C68.

Darensbourg, M. Y., Jimenez, P., Sackett, J. R., Hanckel, J. M., & Kump, R. L. (1982) *J. Am. Chem. Soc. 104*, 1521.

Dykstra, C. E. (1988) *Ab Initio Calculation of the Structures and Properties of Molecules*, Elsevier, New York.

Evangelista-Kirkup, R., Smulevich, G., & Spiro, T. G. (1986) *Biochemistry 25*, 4420.

Flygare, W. H., & Weiss, V. W. (1966) *J. Chem. Phys. 45*, 2785.

Frisch, M. J., Head-Gordon, M., Schlegel, H. B., Raghavachari, K., Binkley, J. S., Gonzalez, C., Defrees, D. J., Fox, D. J., Whiteside, R. A., Seeger, R., Melius, C. F., Baker, J., Martin, R. L., Kahn, L. R., Stewart, J. J. P., Fluder, E. M., Topiol, S., & Pople, J. A. (1988) Gaussian-88, Gaussian, Inc., Pittsburgh, PA.

Fuchsman, W. H., & Appleby, C. A. (1979) *Biochemistry 18*, 1309.

Gray, G. M., & Kraihanzel, C. S. (1983) *J. Organomet. Chem. 241*, 201.

Halle, B., & Wennerström, H. (1981) *J. Magn. Res. 44*, 89.

Hanson, J. C., & Schoenborn, B. P. (1981) *J. Mol. Biol. 153*, 117.

Hawkes, G. E.; Randall, E. W.; Aime, S.; Osella, D., & Elliot, J. E. (1984) *J. Chem. Soc., Dalton Trans.* 279.

Herzfeld, J., & Berger, A. E. (1980) *J. Chem. Phys. 73*, 6021.

Hubbard, P. S. (1970) *J. Chem. Phys. 53*, 985.

Karplus, M., & Pople, J. A. (1963) *J. Chem. Phys. 38*, 2803.

Kerr, E. A., & Yu, N.-T. (1985) *J. Biol. Chem. 260*, 8360.

Kerr, E. A., Mackin, H. C., Yu, N.-T. (1983) *Biochemistry 22*, 4373.

Kintzinger, J.-P. (1981) in *NMR: Basic Principles and Progress* (Diehl, P., Fluck, E., & Kosfeld, R., Eds.) Springer-Verlag, New York.

LaMar, G. N., Dellinger, C. M., & Sankar, S. S. (1985) *Biochem. Biophys. Res. Commun. 128*, 628.

Lee, H. C., & Oldfield, E. (1989) *J. Am. Chem. Soc. 111*, 1584.

Lee, H. C., Gard, J. K., Brown, T. L., & Oldfield, E. (1985) *J. Am. Chem. Soc. 107*, 4087.

Lee, H. C., Cummings, K., Hall, K., Hager, L. P., & Oldfield, E. (1988) *J. Biol. Chem. 263*, 16118.

Lefebvre-Brion, H., Moser, C., Nesbet, R. K., & Ymazaki, M. (1963) *J. Chem. Phys. 38*, 2311.

Lerner, L., & Torchia, D. A. (1986) *J. Am. Chem. Soc. 108*, 4264.

Li, X.-Y., & Spiro, T. G. (1988) *J. Am. Chem. Soc. 110*, 6024.

Lokshin, B. V., Kazaryan, S. G., & Ginzburg, A. G. (1988a)

J. Mol. Structr. 174, 29.
Lokshin, B. V., Kazaryan, S. G., & Ginzburg, A. G. (1988b) *Izv. Akad. Nauk SSSR. Ser. Khim.* 948.
Lovas, F. J., & Tiemann, E. (1974) *J. Phys. Chem. Ref. Data 3*, 609.
Lumpkin, O., Dixon, W. T., & Poser, J. (1979) *Inorg. Chem. 18*, 982.
Maciel, G. E., Shatlock, M. P., Houtchens, R. A., & Caughey, W. S. (1980) *J. Am. Chem. Soc. 102*, 6884.
Matwiyoff, N. A., & Needham, T. E. (1972) *Biochem. Biophys. Res. Commun. 49*, 1158.
Matwiyoff, N. A., Vergamini, P. J., Needham, T. E., Gregg, C. T., Volpe, J. A., & Caughey, W. S. (1973) *J. Am. Chem. Soc. 95*, 4429.
Maxwell, J. C., & Caughey, W. S. (1976) *Biochemistry 15*, 388.
Moon, R. B., & Richards, J. H. (1972a) *Proc. Natl. Acad. Sci. U.S.A. 69*, 2193.
Moon, R. B., & Richards, J. H. (1972b) *J. Am. Chem. Soc. 94*, 5093.
Moon, R. B., & Richards, J. H. (1974) *Biochemistry 13*, 3437.
Moon, R. B., Dill, K., & Richards, J. H. (1977) *Biochemistry 16*, 221.
Morikis, D., Sage, J. T., Rizos, A. K., & Champion, P. M. (1988) *J. Am. Chem. Soc. 110*, 6341.
Morikis, D., Champion, P. M., Springer, B. A., & Sligar, S. G. (1989) *Biochemistry 28*, 4791.
Morishima, I., Hayashi, T., Inubushi, T., Yonezawa, T., & Uemura, S. (1979) *J. Chem. Soc., Chem. Commun.* 483.
Nagai, K., Luisi, B., Shih, D., Miyazaki, G., Imai, K., Poyart, C., De Young, A., Kwiatkowsky, L., Noble, R. W., Lin, S.-H., & Yu, N.-T. (1987) *Nature 329*, 858.
Norvell, J. C., Nunes, A. C., & Schoenborn, B. P. (1975) *Science 190*, 568.
O'Keefe, D. H., Ebel, R. E., Peterson, J. A., Maxwell, J. C., & Caughey, W. S. (1978) *Biochemistry 17*, 5845.
Oldfield, E., Keniry, M. A., Shinoda, S., Schramm, S., Brown, T. L., & Gutowsky, H. S. (1985) *J. Chem. Soc., Chem. Commun.* 791.
Oldfield, E., Guo, K., Augspurger, J. D., & Dykstra, C. E. (1990) *J. Am. Chem. Soc.* (submitted for publication).
Ormos, P., Braunstein, D., Frauenfelder, H., Hong, M. K., Lin, S.-L., Sauke, T. B., & Young, R. D. (1988) *Proc. Natl. Acad. Sci. U.S.A. 85*, 8492.
Parkhurst, L. J., Sima, P., & Goss, D. J. (1980) *Biochemistry 19*, 2688.
Pauling, L., & Coryell, C. D. (1936) *Proc. Natl. Acad. Sci. U.S.A. 22*, 210.
Perkins, T. H. (1982) Ph.D. Thesis, California Institute of Technology.
Perkins, T., Satterlee, J. D., & Richards, J. H. (1983) *J. Am. Chem. Soc. 105*, 1350.
Perutz, M. F. (1989) *Trends Biochem. Sci. 14*, 42.
Perutz, M. F., & Lehmann, H. (1968) *Nature 219*, 902.
Phillips, S. E. V., & Schoenborn, B. P. (1981) *Nature 292*, 81.
Ramsden, J., & Spiro, T. G. (1989) *Biochemistry, 28*, 3125.
Reuben, J., & Luz, Z. (1976) *J. Phys. Chem. 80*, 1357.
Richardson, J. W. (1960) *Rev. Mod. Phys. 32*, 461.
Romero-Herrera, A. E., Goodman, M., Dene, H., Bartnicki, D. E., & Mizukami, H. (1981) *J. Mol. Evol. 17*, 140.
Rosenblum, B., & Nethercot, A. H., Jr. (1957) *J. Chem. Phys. 27*, 828.
Satterlee, J. D. (1983) *Inorg. Chim. Acta 79*, 170.
Satterlee, J. D., Teintze, M., & Richards, J. H. (1978) *Biochemistry 17*, 1456.
Seamonds, B., McCray, J. A., Parkhurst, L. J., & Smith, P. D. (1976) *J. Biol. Chem. 251*, 2579.
Smith, M. L., Paul, J., Ohlsson, P.I., & Paul, K. G. (1984) *Biochemistry 23*, 6776.
Springer, B. A., & Sligar, S. G. (1987) *Proc. Natl. Acad. Sci. U.S.A. 84*, 8961.
Springer, B. A., Egeberg, K. S., Sligar, S. G., Rohlfs, R. J., Mathews, A. J., & Olson, J. S. (1989) *J. Biol. Chem. 264*, 3057.
Stryer, L. (1988) *Biochemistry*, pp 148–150, Freeman, New York.
Tsubaki, M., Srivastava, R. B., & Yu, N.-T. (1982) *Biochemistry 21*, 1132.
Tucker, P. W., Phillips, S. E. V., Perutz, M. F., Houtchens, R., & Caughey, W. S. (1978) *Proc. Natl. Acad. Sci. U.S.A. 75*, 1076.
Uno, T., Nishimura, Y., Makino, R., Iizuka, T., Ishimura, Y., & Tsuboi, M. (1985) *J. Biol. Chem. 260*, 2023.
Uno, T., Nishimura, Y., & Tsuboi, M. (1987) *J. Biol. Chem. 262*, 4549.
Walter, T. H., Reven, L., & Oldfield, E. (1989) *J. Phys. Chem. 93*, 1320.
Waterman, M. R., & Stengal, P. (1974) *Biochim. Biophys. Acta 359*, 401.
Wilbur, D. J., & Allerhand, A. (1977) *J. Biol. Chem. 252*, 4968.
Yu, N.-T., Kerr, E. A., Ward, B., & Chang, C. K. (1983) *Biochemistry 22*, 4534.
Zamyatnin, A. A. (1972) *Prog. Biophys. 24*, 107.